博士論文

Analysis of *DWARF14*, a strigolactone receptor, and its homologs

(ストリゴラクトン受容体をコードする *DWARF14* 遺伝子とそのホモログの解析)

亀岡　啓

Contents

Abstract

植物は固着性の生活様式をとるため、周囲の環境に応じてその形態や生理状態を変化させる必要がある。この様な応答において、植物ホルモンとその受容体が中心的な役割を担う。植物ホルモンは合成や輸送を環境からの刺激に制御されて細胞間を移行する。そして、受容体が応答に必要な細胞で植物ホルモンと結合することで、個体として協調的な反応が誘導される。

ストリゴラクトンは腋芽伸長の抑制を始め様々な生理作用をもつ植物ホルモンであり、その受容体は DWARF14 (D14)であると推定されている。D14 がストリゴラクトンと結合すると D14, DWARF3 (D3), DWARF53(D53)の三者が相互作用し、D53 が分解されることによって下流の応答が誘導される。*D14* とそのホモログは *D14* ファミリーと呼ばれる小さな遺伝子ファミリーを形成する。イネは *D14, D14LIKE* (*D14L*), *D14 LIKE2a* (*D14L2a*) , *D14 LIKE2b* (*D14L2b*)の 4 遺伝子をもつが、これまでに報告されている研究から、*D14* ファミリーの遺伝子はそれぞれ興味深い特徴をもつことが示唆されている。そこで本研究では、*D14* ファミリー遺伝子について機能解析を行った。

DWARF14 (D14)タンパク質は師管輸送される

プロテオーム解析により、D14 タンパク質がイネの師管液から検出されることが報告された。この結果は、D14 タンパク質が師管を輸送される可能性を示唆している。近年、タンパク質の細胞間輸送が植物の形態形成において重要な役割を担うことが明らかになってきたが、植物ホルモンの信号伝達経路で働くタンパク質が細胞間を輸送される例は知られていない。そこで、D14 タンパク質の師管輸送について解析した。

まず、mRNA の発現パターンを調べた。*D14* mRNA は維管束と葉原基で発現しており、腋芽メリステムでは発現がみられなかった。また、維管束内では師部伴細胞と木部柔組織で発現していた。次に、師管に D14 タンパク質があるか検証するために、*D14* プロモーターの制御下で D14:GFP 融合タンパク質を導入した系統(*pD14::D14:GFP* 系統)を用いて師部を観察した。すると、mRNA が発現している伴細胞に加え、師管でも D14 タンパク質のシグナルが検出された。さらに、この系統では、mRNA の発現がみられなかった腋芽メリステムでも GFP 蛍光が観察された。これは、D14:GFP 融合タンパク質が腋芽メリステムへ輸送されたためである可能性が考えられる。そこで、同じプロモーターで D14 と 3 つの GFP が繋がれたタンパク質を導入した系統(*pD14::D14:3xGFP* 系統)を作成した。D14:3xGFP 融合タンパク質は分子量が大きいため、細胞間を輸送されない。この系統では腋芽メリステムに GFP 蛍光がみられなかったことから、*pD14::D14:GFP* 系統の腋芽メリステムで観察された D14:GFP 融合タンパク質は、細胞間を輸送されてきたものであることが確認された。これ

らの結果から、D14 タンパク質は師管を通り腋芽へ輸送されることが明らかとなった。また、ストリゴラクトン欠損変異体背景の *pD14::D14:GFP* 系統でも、腋芽メリステムに GFP 蛍光が観察された。このことから、ストリゴラクトンは D14 輸送に必要ないことも示された。

さらに、D14 輸送が腋芽伸長を制御するか検証するため、*d14* 変異体背景の *pD14::D14:3xGFP* 系統の表現型を解析した。この系統では、腋芽伸長が野生型植物と同程度に抑制されていたため、D14 輸送は腋芽伸長の抑制に必須ではないことが示された。また、光による腋芽伸長の調節への寄与を検証したが、D14 輸送はこの現象にも関与していなかった。

しかし、エンドウを用いた接ぎ木実験では、エンドウの *D14* ホモログ変異体である *rms3* 変異体の腋芽は、野生型台木を接ぎ木されることによって抑制されることが報告された。この結果は、接ぎ木間を輸送された D14 タンパク質が腋芽伸長を抑制した可能性を示唆する。

以上の結果から、D14 は師管を介して腋芽に輸送されることが明らかとなった。また、D14 輸送は腋芽伸長抑制に必須ではないが、腋芽伸長を制御するポテンシャルをもつことも示唆された。

DWARF14 LIKE (D14L)はストリゴラクトン信号伝達以外の経路で暗黒条件下のメソコチル伸長を抑制する

ストリゴラクトンはイネで暗所形態形成に関与し、暗黒条件下でメソコチル伸長を抑制する。そのため、ストリゴラクトン関連遺伝子の変異体では、暗所で野生型植物に比べてメソコチルが長くなる。これらの変異体の中で、*d3* 変異体は他の変異体に比べて顕著に強い表現型を示す。これは、*D3* がストリゴラクトン経路以外でも働くことを示唆している。シロイヌナズナの *D14L* オーソログである *KAI2* は、*D3* と共にストリゴラクトン信号伝達以外の経路で光形態形成を制御することが示されていることから、メソコチルの伸長制御においても *D14L* が関与しているのではないかと考えた。

そこで、RNAi 法により *D14L* をノックダウンした系統(*D14L* RNAi 系統)を作成し、メソコチルの表現型を観察した。この系統では、他のストリゴラクトン関連遺伝子の変異体と同様に、明所ではメソコチルの表現型はみられなかったのに対し、暗所でメソコチル伸長の促進が観察された。また、*d14* 変異体のメソコチル伸長はストリゴラクトン合成アナログの投与により抑制されず、*D14L* RNAi 系統では抑制されたことから、*D14L* はストリゴラクトン信号伝達以外の経路でメソコチル伸長を制御することが示された。また、*d14* 変異体背景で *D14L* をノックダウンした系統のメソコチルは、*d14* 変異体のメソコチルに比べて有意に長かった。これは、*D14* と *D14L* がメソコチル伸長抑制に対して相加的に働いていることを示し、また、*d3* 変異体でのみ観察される強いメソコチル伸長促進の表現型が、*D14L* の機能によることを示唆している。

以上の結果から、*D14* がストリゴラクトン経路で働くのに対し、*D14L* は別経路で働くことが示された。D14 がストリゴラクトンの受容体であると推定されていることから、D14L も未知の植物ホルモンの受容体である可能性も考えられる。

DWARF14 LIKE2 (*D14L2*)はアーバスキュラー菌根菌(AM 菌)によって発現誘導される

ストリゴラクトンは植物ホルモンとしての作用以外に、AM 菌の菌糸分岐を促進する活性をもつ。そのため、ストリゴラクトンの合成経路で働く遺伝子の変異体では共生が抑制される。逆に、*d14* 変異体では、フィードバックによって野生型植物より多くストリゴラクトンを合成、分泌しているため、共生率が上昇する。しかし、*d3* 変異体では、*d14* 変異体同様にストリゴラクトンを多く分泌しているにも関わらず、共生は著しく抑制された。これは *D3* が *D14* とストリゴラクトン信号伝達以外の経路で AM 菌感染を制御しているためだと考えられる。

そこで、ストリゴラクトン信号伝達以外の経路で働くことが示された *D14L* がこの現象にも寄与しているのではないかと考え、*D14L* RNAi 系統での AM 菌共生の表現型を観察した。しかし、野生型植物と *D14L* RNAi 系統の間で有意な共生率の差はみられなかった。また、*D14* と *D14L* が冗長的に働いている可能性も考えられるため、*d14* 変異体背景の *D14L* RNAi 系統でも表現型を観察したが、この系統では、*d14* 変異体と同様の高い共生率を示した。これらの結果から、*D14L* は AM 菌共生の制御に寄与していないことが示された。

一方、トランスクリプトーム解析から、AM 菌によって *D14L2* の発現が誘導されることが報告された。そこで、AM 菌共生における *D14L2* の機能を解明するための第一歩として、この発現誘導を詳細に観察した。

まず、*D14L2a* プロモーターの制御下で YFP を発現する系統を作製し、AM 菌接種時の *D14L2a* mRNA の発現パターンを観察した。*D14L2a* の発現は AM 菌共生の早い段階から誘導されており、菌糸が根に侵入する前の段階でも発現がみられた。

次に、*D14L2* 発現誘導と、既知の AM 菌共生に必要な遺伝子との関係を調べた。植物は共通感染経路と呼ばれる一群の遺伝子によって AM 菌を感知し、下流の共生特異的な遺伝子発現を誘導することが知られている。しかし、*D14L2* の発現は共通感染経路で働く遺伝子の変異体でも野生型植物と同様に誘導された。それに対して、*d3* 変異体では *D14L2* の発現誘導はみられなかった。これらの結果は、*D3* が共通感染経路とは独立して働き、AM 菌共生を制御していることを示唆する。

D3 は様々な形質の制御において *D14* ファミリー遺伝子と共に働くことが知られている。本研究において *D3* による AM 菌共生制御に *D14* と *D14L* が関与しないこと、下流で *D14L2* が発現誘導されることが示されたことから、*D14L2* が *D3* と共に AM 菌共生を制御している可能性も考えられる。

以上のように、本研究では *D14* ファミリー遺伝子について、新たな機能や特徴を明らかにした。植物ホルモン受容体による応答制御の仕組みとして、受容体タンパク質が細胞間を輸送されることが示されたことや、ホモログ間で別個のリガンドを受容して信号伝達を行っている可能性が示唆されたことは興味深い。これらの現象の全容を明らかにすることで、植物の環境に柔軟に適応する能力の理解に繋がると考えられる。

1. General Introduction

Plants adapt their developmental and physiological conditions to surrounding environment. In this response, plant hormones play crucial roles. Environmental signals are transduced between cells by the transport of plant hormones whose biosynthesis and transport are regulated by environmental cues. The downstream events of plant hormone signaling are triggered by the perception of plant hormones by the receptors which are expressed in the cells required for the environmental response. Thus, environmental responses are induced coordinately in whole plant.

Strigolactones (SLs) are a class of plant hormones. The first reported function of SLs as plant hormone is suppression of shoot branching (Gomez-Roldan et al., 2008; Umehara et al., 2008). Since then, a growing number of additional biological functions of SLs have been discovered (Seto et al., 2012).

It has been shown that the biosynthesis and the transport of SLs are controlled by the availability of nutrients in soil, such as phosphate and nitrate (Kretzschmar et al., 2012; Umehara et al., 2010; Xie et al., 2014). The regulation of shoot branching, root architecture, and the senescence in response to nutrients is impaired in SL deficient and insensitive mutants (de Jong et al., 2014; Mayzlish-Gati et al., 2012; Umehara et al., 2010; Yamada et al., 2014). *DWARF27* (*D27*), *CAROTENOID CLEAVAGE DIOXYGENASE 7* (*CCD7*), *CAROTENOID CLEAVAGE DIOXYGENASE 8* (*CCD8*), and *MORE AXILLARY GROWTH 1* (*MAX1*) function in SL biosynthesis (Abe et al., 2014; Alder et al., 2012; Gomez-Roldan et al., 2008; Lin et al., 2009; Scaffidi et al., 2013; Seto et al., 2014; Umehara et al., 2008; Zhang et al., 2014b;) (Fig. 1.1). PLEIOTROPIC DRUG RESISTANCE1 (PDR1) was identified as an efflux transporter

of SLs in petunia and *Nicotiana tabacum* (Kretzschmar et al., 2012; Xie et al., 2014). These genes are upregulated under nutrient deficient conditions.

DWARF14 (D14) is a putative SL receptor. *D14*, *DWARF3* (*D3*), and *DWARF53* (*D53*) work in SL signaling pathway (Arite et al., 2009; Hamiaux et al., 2012; Jiang et al., 2013; Umehara et al., 2008; Zhou et al., 2013). *D14* and *D3* encode an α/β-fold hydrolase protein, and an F-box protein, respectively. Mutants in these genes are insensitive to SLs (Arite et al., 2009; Umehara et al., 2008).Upon binding of SLs to D14, a conformation change happens to D14 and a complex of SL-bound D14, D3, and D53, a Clp ATPase protein, is formed (Hamiaux et al., 2012; Jiang et al., 2013; Zhou et al., 2013). Then, D53 is polyubiquitinated by D3 and degraded *via* 26S proteasome pathway. The *d53* mutant in which D53 protein is not degraded by SLs is insensitive to SLs (Jiang et al., 2013; Zhou et al., 2013). These observations demonstrate that D53 works as a repressor of SL signaling and that the degradation of D53 induces the cascade of downstream events (Jiang et al., 2013; Zhou et al., 2013) (Fig. 1.2). D14 has a SL cleavage activity (Hamiaux et al., 2012) (Fig. 1.2). Therefore, it is possible that the product of the cleavage by D14 is the active form of the hormone. The fact that SL perception by D14 induces the degradation of D53, however, strongly suggests a notion that D14 is a SL receptor. In this thesis, I describe D14 as a SL receptor.

Four *D14* homologs, *D14*, *D14 LIKE* (*D14L*), *D14 LIKE2a* (*D14L2a*), and *D14 LIKE2b* (*D14L2b*), are found in the rice genome (Table 1.1). *D14* homologs are conserved in land plants, which are called *D14* family. They are classified into two clades: *D14* and *D14LIKE* (*D14L*). The *D14* clade is further sub-divided into the core *D14* and the *D14 LIKE 2* (*DLK2*) subclades (Delaux et al. 2012; Waters et al., 2012) (Fig. 1.3).

Several interesting features of *D14* family genes have been reported. First, D14 family proteins are detected in phloem sap of rice and Arabidopsis in proteome analysis (Aki et al., 2008; Batailler et al., 2012). Although D14 family proteins were not examined in detail in these reports, a possibility that the distributions of D14 family proteins are regulated by phloem transport was suggested. Second, it has been shown that *D14L* homolog in Arabidopsis is responsible for karrikin signaling. Karrikins are chemicals found in smoke (Flematti et al., 2007). They stimulate seed germination and enhance photomorphogenesis (Flematti et al., 2007; Nelson et al., 2010). *D14L* homolog was identified as the causal gene of *karrikin insensitive2* (*kai2*) mutant in Arabidopsis (Waters et al., 2012) (Table 1.1). Karrikins directly bind to KAI2 (Guo et al., 2013). Moreover, it was shown that *KAI2* does not function in SL signaling pathway (Scaffidi et al., 2014). These results imply that proteins in D14 and D14L clade recognize distinct ligands. Furthermore, it was found that the mRNA expression of *D14L2a* and *D14L2b* is strongly induced by Arbuscular mycorrhizal (AM) fungi (Hata et al., personal communication). This implies the possibility that *D14L2a* and *D14L2b* are involved in AM fungi symbiosis. In Arabidopsis, the *dlk2* mutant was analyzed but no visible phenotype was detected (Waters et al., 2012).

These features of *D14* family genes may reflect the existence of novel mechanisms in which plant hormone receptors regulate plant hormone signaling. To understand the basis of these unknown regulatory systems, I analyzed these features of *D14* family genes. In Chapter 2, I characterize the D14 protein transport. I show that D14 is transported to axillary meristems through phloem and that the D14 transport is not essential to regulate shoot branching. In Chapter 3, I show *D14L* function in skotomorphogenesis in rice. *D14* and *D14L* work additively for the suppression of

mesocotyl elongation under dark conditions. *D14* functions in the SL signaling pathway, while *D14L* functions in an as yet unknown SL independent pathway. In Chapter 4, I show that *D14* and *D14L* are not involved in the regulation of the symbiosis with AM fungi. Moreover, I describe that the genetic pathway of the induction of *D14L2a* and *D14L2b* expression by AM fungi.

Table 1.1.*D14* family genes and genes in SL signaling pathway.

	Rice	Arabidopsis	Pea
D14 family genes	*D14*	*AtD14*	*RMS3*
	D14L	*KAI2*	
	D14L2a, D14L2b	*DLK2*	
F-box	*D3*	*MAX2*	*RMS4*
Clp ATPase	*D53*		

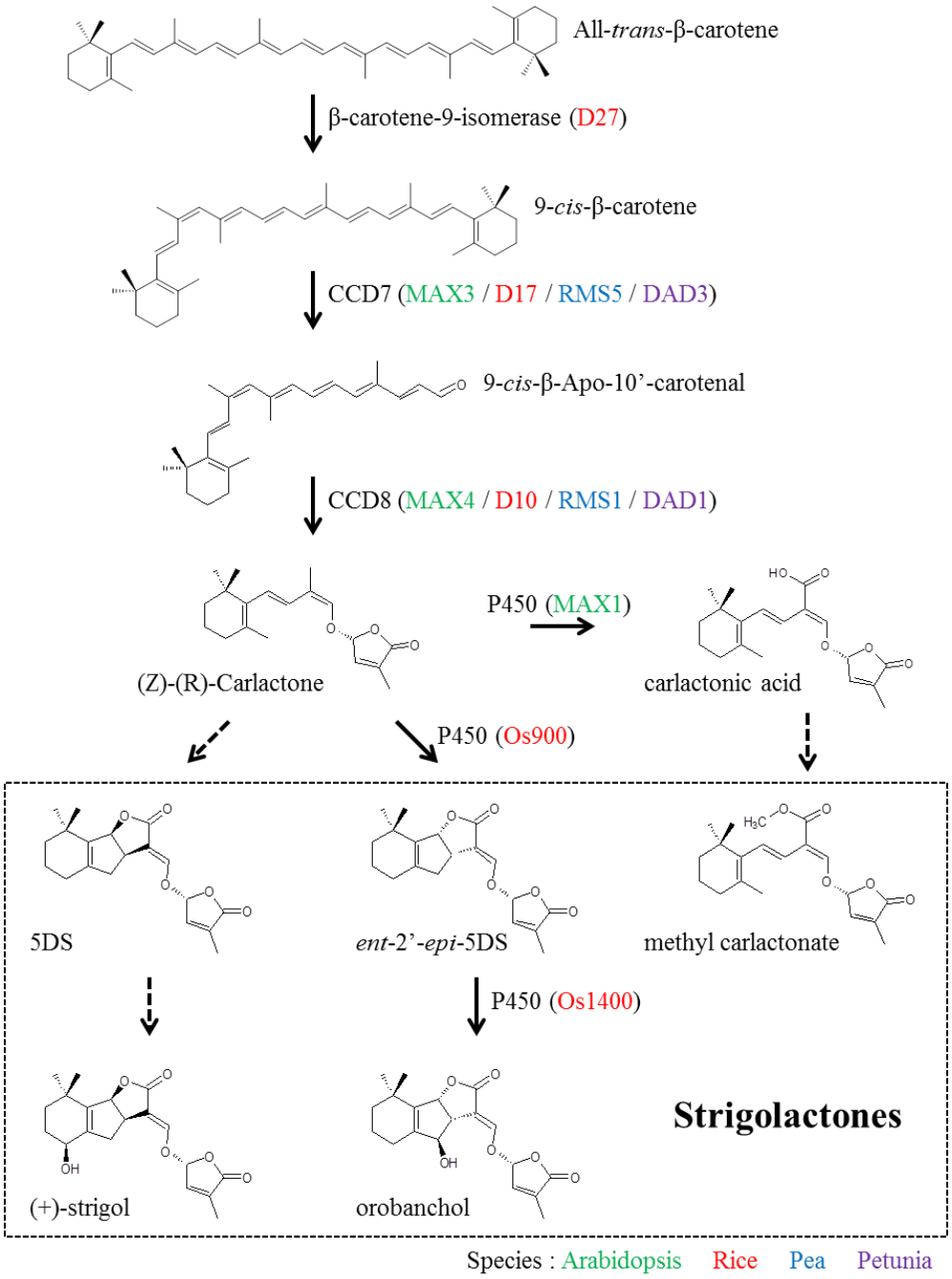

Figure 1.1. Strigolactone biosynthesis pathway.

SLs are synthesized from carotenoid. D27, CCD7, and CCD8 catalyze the conversion from all-*trans*-β-carotenoid to (Z)-(R)-carlactone. MAX1 is involved in the transformation from (Z)-(R)-carlactone to SLs. In rice, two MAX1 homologs catalyze distinct steps from (Z)-(R)-carlactone to orobanchol.Allows of s broken line indicate perspective reactions. Green, red, blue, and purple characters indicate genes of Arabidopsis, rice, pea and petunia, respectively.

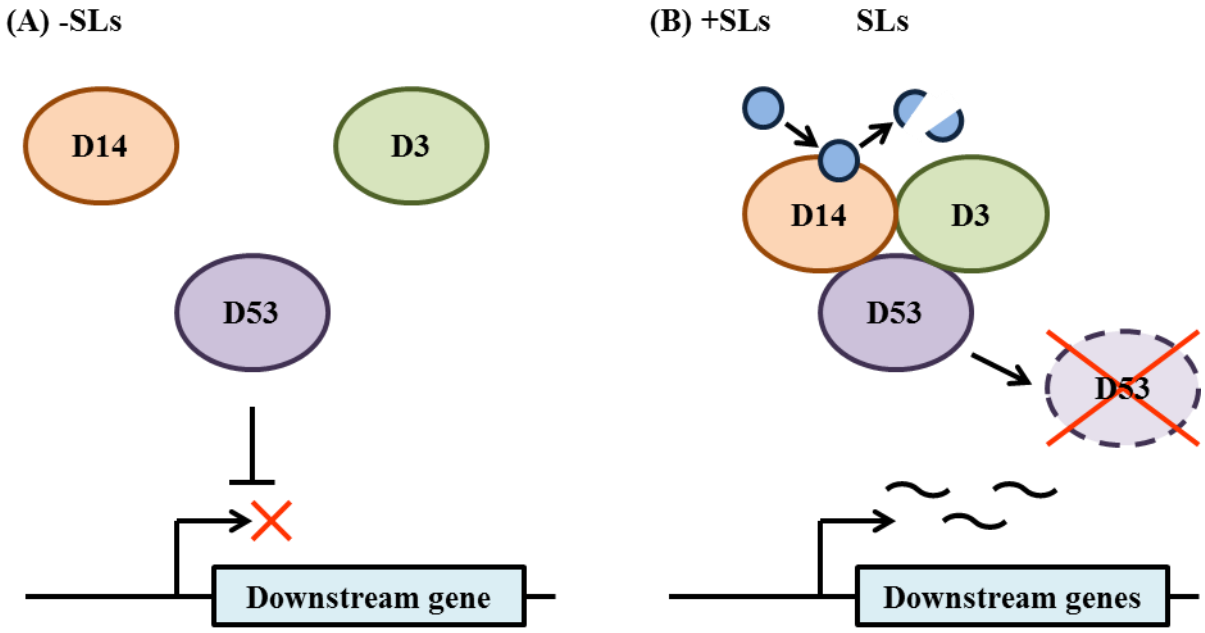

Figure 1.2. Strigolactone signaling pathway.

(A) While SLs are absence, D53 suppresses SL signaling. (B) When SLs are perceived by D14, the interaction between D14, D3, and D53 are induced, and subsequently, D53 is polyubiduitinized by D3 and degraded via 26S proteasome pathway. Then, the cascade of downstream starts. SLs are cleaved by D14.

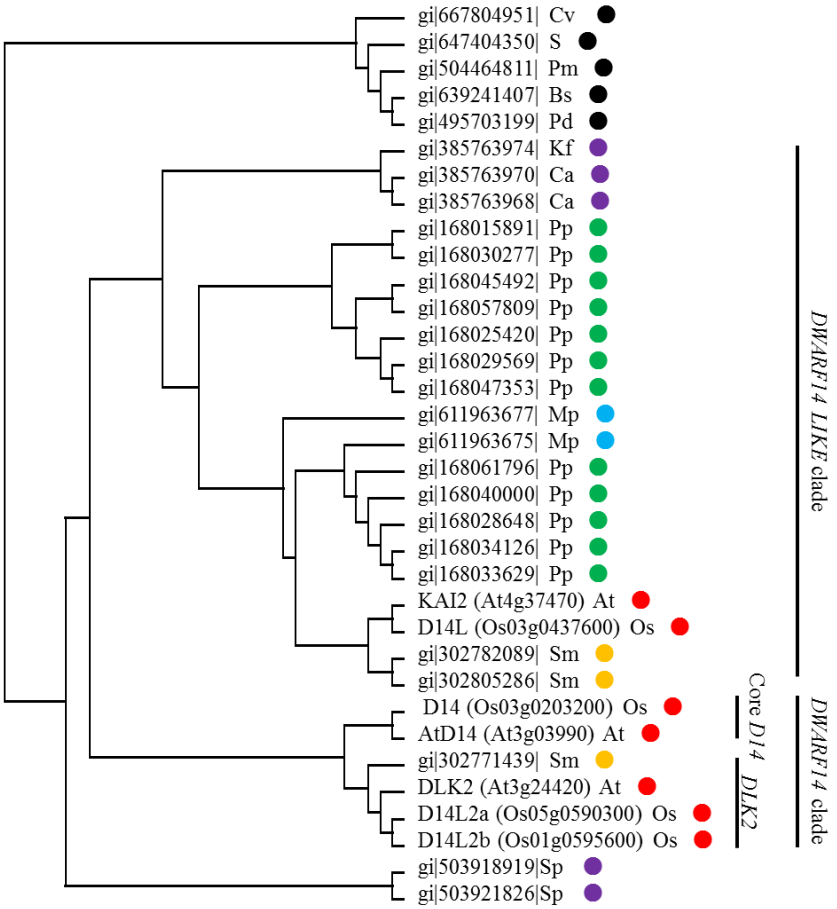

Figure 1.3. Phylogeny of *D14* family .

Maximum-likelihood (ML) tree of D14 family. *D14* family genes are classified into two clades: *D14* and *D14LIKE* (*D14L*). The *D14* clade is further subdivided into the core *D14* and the *D14 LIKE 2* (*DLK2*) subclades. Genes in *D14* clade were not found from mosses, liverworts, and charophytes. Circles colored with red, yellow, green, blue, purple, and black indicate Angiosperm, lycophyte, moss, liverwort, charophyte, and bacterium, respectively. Os, Oryza sativa; At, Arabisopsis thaliana; Sm, Selaginella moellendorffii; Pp, Physcomitrella patens; Mp, Marchantia polymorpha; Ca, Chlorokybus atmophyticus; Kf, Klebsormidium flaccidum; Sp, Streptomyces pratensis; Bs, Bacillus subtilis; Cv, Cystobacter violaceus; S, Sporosarcina sp.; Pm, Paenibacillus mucilaginosus; Pd, Planococcus donghaensis. Sequences were obtained with BLASTP searches of GenBank protein databases using the rice D14 amino acid sequence as a query (http://www.ncbi.nlm.nih.gov). Full-length sequences were then aligned using Clustal W(http://clustalw.ddbj.nig.ac.jp/) using the default settings. ML tree was sound with PhyML 3.0 (http://atgc.lirmm.fr/phyml/) /) using the default settings. The tree is rooted with bacterial RsbQ sequences.

2. DWARF 14 protein is transported through phloem

2.1. Introduction

Cell-to-cell communication is essential for multicellular organisms to coordinate the growth of the cells. Transport of signaling molecules plays critical rolls for the cell-to-cell communication. In plants, two distinct systems are used for the transport of signaling molecules (Bloemendal and Kück, 2013).

The first is apoplastic transport. Signaling molecules secreted from the cells where they are synthesized, are transported through apoplast, and perceived by the receptors in the cells where they exert their functions (Endo et al., 2014; Santner et al., 2009). Many plant hormones and peptide signals are transported by this system (Bloemendal and Kück, 2013).

The second is symplastic transport. The cytoplasm of plant cells are connected with neighboring cells *via* channels called plasmodesmata (PD) (Bloemendal and Kück, 2013). Signaling molecules are transported through PD. It is well described that short-distance transport of transcription factors play crucial rolls in tissue patterning and organ formation (Han et al., 2014). Disruption of PD permeability causes defects in many aspects of development, indicating the importance of the symplastic transport (De Storme et al., 2014; Han et al., 2014; Hisanaga et al., 2014). Phloem is the organ for the long-distance symplastic transport. Phloem sap contains many kinds of macromolecules, such as plant hormones, proteins and RNAs (Turgeon et al., 2009). Among them, it has been shown that FT/Hd3a protein functions as a signaling molecule. The expression of *FT*/*Hd3a* mRNA is stimulated by environmental and developmental cues in phloem

companion cells (CCs) in leaves and the proteins are transported to the shoot apical meristem through the phloem to induce flowering (Liu et al., 2013).

SLs are transported from roots to shoots and suppress shoot branching (Bainbridge et al., 2005; Beveridge et al., 1996; Booker et al., 2004; Booker et al., 2005; Foo et al., 2001; Johnson et al., 2006; Morris et al., 2001; Simons et al., 2007). SLs are thought to be transported through apoplast. PDR1, an efflux transporter of SLs, is involved in the transport (Kretzschmar et al., 2012; Xie et al., 2014). Although whole aspects of SL transport remain to be unclear, it is reasonable to assume that environmental and internal signals are transmitted through the SL transport (Umehara et al., 2010). Moreover, D14 proteins were detected in phloem sap of rice and Arabidopsis by proteome analysis (Aki et al., 2008; Batailler et al., 2012). It implies a possibility that D14 is also transported for a long distance and functions as a signaling molecule.

In this chapter, I analyzed the D14 transport. I show that the D14 protein is transported to axillary meristems through phloem. To my knowledge, this is the first case that a component in a plant hormone signaling pathway is shown to be mobile.

2.2. Materials and methods

Plant materials and growth conditions

The *d10-2* was described previously (Umehara et al., 2008). *d14-1* mutant was backcrossed four or five times to Nipponbare and used in this study.

Sterilized seeds were germinated in water for 1 day under the dark condition and grown on the solidified hydroponic culture media (Umehara et al., 2008) for 7 days in

an incubator (16h light, 8h dark at 25° C). To analyze the responses to light intensity, they were grown in a strong light condition (20,000 lux) or a weak light condition (10,000 lux) on soil in an incubator (14h light at 28° C, 10h dark at 25° C)

Plasmid construction and transgenic rice production

To construct *pD14::D14:GFP*, ca. 4.5 kbp region including *D14* promoter and *D14* ORF were amplified using a primer set, D14 F and D14 R. The PCR fragment was introduced into the pGWB4 expression vector (Nakagawa et al. 2007) using the Gateway system (Invitrogen). To construct *pD14::D14:3xGFP*, *pD14::D14:GFP* Δ STOP, *GFP* Δ STOP, *GFP* region were amplified from *pD14::D14:GFP* vector, using primer sets, D14 F2 and GFP R2, GFP F and GFP R2, and GFP F and GFP R, respectively. After sub-cloned into pBluescript SK, they were cloned into pBI 101.2 vector. To construct *pHSP::GFP*, promoter region of *OsHSP101* (Chang et al., 2007) were amplified using a premer set, OsHSP F and OsHSP R. After sub-cloned into pBluescript SK, it was cloned into pBI 101.2 together with the GFP fragment. Transformation of rice was carried out as described by Nakagawa et al. (2002). Primer sets used for construction were described in Table 2.1.

***In situ* hybridization**

In situ hybridization was performed as described by Kouchi et al. (1995). The full length *D14* cDNA was amplified using a primer set, D14 F and D14 R. The PCR fragment was cloned into pENTR/D-TOPO (Life Technologies), and cut by Hind III. 3’

region of the fragment was used as a template to make the *D14* antisense probe. *GFP* fragment cloned into pBluescript SK as described above was used as a template to make the *GFP* antisense probes.

Immunostaining

Immunostaining was performed as described by Yamaji et al. (2007). Samples were sectioned 100 μm thick. Anti-GFP, Rabbit IgG Fraction, polyclonal (life technologies) and Alexa Fluor 555 goat anti-rabbit IgG (Molecular Probes) were used as primary and secondary antibodies, respectively. Fluorescence of secondary antibody and auto-fluorescence of cell wall were observed with a confocal laser-scanning microscopy (LSM700; Carl Zeiss).

Western blotting

The synthetic peptide C+SVNPDHFDFRRYDN (108aa-121aa of OsD14) was used to raise anti-D14 polyclonal antibodies in rabbit.

Total proteins were extracted from the basal part of rice seedlings using an extraction buffer (50 mM Tris HCl, pH 7.5, 150mM NaCl, 10% glycerol, protease inhibitor cocktail). After centrifugation (15,000 rpm at 4° C), the supernatant was collected. Samples were resolved by SDS-PAGE, and transferred to Amersham Hybond P membrane (GE Healthcare). After blocking with 5% skim milk in TBS-T buffer (0.02% Tween-20), the membrane was incubated with Anti-GFP Tag antibody (AnaSpec) or anti-D14 antibody (1:1000 dilution in Can Get Signal; Toyobo), and then

with Anti-Rabbit IgG, HRP-Linked Whole Ab Donkey (GE Healthcare) (1:1000 dilution in Can Get Signal; Toyobo). The signal was detected by using ECL Prime Western Blotting Detection System and ImageQuant LAS 4000mini (GE Healthcare).

GFP fluorescence observation

The basal parts of rice seedlings were mounted in the 7% agarose gel, and sectioned to 50 μm thick by using a microslicer. GFP fluorescence was observed with a confocal laser-scanning microscopy (FV1000; Olympus).

Quantitative reverse transcription-PCR

Total RNA was extracted from leaf blades using Plant RNA Isolation kit (Agilent Technologies). After DNase I treatment, first-strand cDNA was synthesized using Super Script III reverse transcriptase (Life Technologies). The primer sets used for qPCR were described in Table 2.1. PCR was performed with SYBR green using Light Cycler 480 System II (Roche Applied Science).

2.3. Results

2.3.1. Spatial expression pattern of *D14* mRNA

Although the broad spatial expression pattern of *D14* mRNA was reported in rice and Arabidopsis previously (Arite et al., 2009; Chevalier et al., 2014), details have not been

described yet. Since precise determination of the sites where *D14* mRNA is expressed is prerequisite to analyze D14 protein movement, I investigated *D14* mRNA distribution by *in situ* hybridization. *D14* mRNA was expressed in vascular bundles and leaf primordia (Fig. 2.1). While *D14* mRNA was expressed in most cells in leaf primordia, the expression was restricted to the vascular bundles in mature leaves (Fig. 2.1). Expression of *D14* mRNA was hardly detected in axillary meristems (Fig. 2.1 A, B).

In vascular bundles, *D14* mRNA was expressed both in phloem and xylem (Fig. 2.1 C). The phloem is composed of sieve elements (SEs), companion cells (CCs) and parenchyma cells. Mature SEs are highly specialized for transporting phloem sap. They lose their nuclei and ribosomes (Furuta et al., 2014; Turgeon et al., 2009). Therefore, proteins in phloem sap are thought to be synthesized in CCs linked to the SEs or in immature SEs. *D14* mRNA was expressed in CCs (Fig. 2.1 C). The expression of *D14* in CCs is consistent with the results of proteome analysis that showed D14 protein is contained in the phloem sap.

2.3.2. D14 protein is contained in rice phloem sap

To observe D14 protein distribution, *pD14::D14:GFP,* which produces D14:GFP fusion protein under the control of the native *D14* promoter, was introduced to WT rice. Two transgenic lines showing strong fluorescence were chosen from twenty independent lines for further analysis. First, I examined whether D14 protein is contained in the rice phloem sap by using immunostaining with anti-GFP antibody. The specificity of this antibody was confirmed because no signal was observed in WT plants (Fig. 2.2 A). In *pD14::D14:GFP* lines, the GFP signal was observed not only in CCs

where *D14* mRNA was expressed, but also in SEs (Fig. 2.2 B). The signal observed in SEs is that of D14:GFP fusion protein but not that of free GFP derived from degraded D14:GFP fusion protein, because free GFP was not detected in the extracts from *pD14::D14:GFP* lines by the western blotting experiment (Fig. 2.2 D). These results demonstrate that the D14 protein is contained in the phloem sap.

Phloem proteins synthesized in CCs are transported to SEs through PD (Turgeon et al., 2009). Molecules larger than the exclusion size limit are not able to pass the PD (Fisher and Cash-Clark, 2000). To confirm that D14 protein is transported from CCs to SEs, I generated *pD14::D14:3xGFP* lines which produce D14 protein fused with three tandem repeats of GFP. Two transgenic lines in which strong fluorescence was observed were chosen from 27 independent lines for analysis. In these two lines, GFP signal was not detected in SEs (Fig. 2.2 C). It suggests that D14 protein is transported from CCs to SEs through PD.

2.3.3. D14 protein is transported to axillary buds

SLs suppress axillary bud outgrowth (Gomez-Roldan et al., 2008; Umehara et al., 2008). Therefore, to test a possibility that the transport of D14 protein is involved in the control of axillary bud growth, I analyzed D14 protein movement in axillary buds using *pD14::D14:GFP* and *pD14::D14:3xGFP* lines. mRNA expression patterns of the introduced genes in these lines were determined by *in situ* hybridization experiment with *GFP* anti-sense probe. The localization of the *GFP* mRNA signal in these lines was indistinguishable from that of endogenous *D14* mRNA (Fig. 2.3 A, B). In *pD14::D14:GFP* lines, GFP fluorescence was observed in axillary meristems in spite

that *D14:GFP* mRNA was hardly detected (Fig 2.3 A, C-E). It suggests that D14:GFP fusion protein is transported to axillary meristems. On the other hand, GFP fluorescence was restricted to the vascular bundles and the basal part of the meristems in *pD14::D14:3xGFP* lines (Fig. 2.3 F-H). Taken together, I concluded that D14 protein is transported to the axillary meristems.

The fluorescence of GFP was not detected in leaf primordia in *pD14::D14:3xGFP* lines where both endogenous *D14* mRNA and *D14:3xGFP* mRNA were expressed (Fig. 2.1 B, 2.3 B, F-H). It implies the occurrence of post-transcriptional regulation to *D14*. On the other hand, the fluorescence of GFP was detected in leaf primordia in *pD14::D14:GFP* lines (Fig. 2.3 C-E). This suggests that D14 protein is transported to leaf primordia, too.

2.3.4. Strigolactones are not required for D14 transport

Next, I tested if SLs influence D14 movement. *pD14::D14:GFP* was introduced in *d10-2*, a SL deficient mutant. GFP fluorescence was observed in axillary meristems and leaf primordia in these transgenic lines in a similar pattern observed in *pD14::D14:GFP* lines of WT background (Fig. 2.3 C-E, Fig. 2.4). This indicates that SLs are not required for the D14 transport.

2.3.5. D14 transport is not essential to suppress tillering

To analyze the contribution of the D14 protein transport to *D14* function, *pD14::D14:GFP* and *pD14::D14:3xGFP* were introduced to *d14* mutant. For each

construct, one line, in which the expression level of the transgene was comparable to that of endogenous *D14*, was chosen from more than ten independent lines for analysis (Fig. 2.5 F). Plants of the selected lines were grown in a hydroponic culture system and their tillering phenotype was analyzed. In this hydroponic calture system, mutant phenotype was complemented in both *pD14::D14:GFP* and *pD14::D14:3xGFP* lines (Fig. 2.5 A-E). This implies that both mobile D14:GFP fusion protein and the immobile D14:3xGFP fusion protein are functional to control tillering. To rule out a possibility that the complementation in *pD14::D14:3xGFP* lines was caused by the D14 protein derived from degradation of D14:3xGFP fusion protein, I carried out western blotting with anti-D14 antibody. D14 protein was not detected in the extracts of *pD14::D14:3xGFP* lines (Fig. 2.5 G). These results suggest that D14 protein trafficking is not prerequisite for *D14* function to suppress the outgrowth of axillary buds, at least under this condition.

2.3.6. SLs regulate tillering in response to the intensity of light but D14 transport is not related to the light response

To reveal the biological significance of D14 transport, I investigated the possibility that D14 transport may be involved in the responses to environmental conditions. Transcriptome analysis showed that strong light decreased *D14* mRNA expression level (Osuna et al., 2007). Moreover, it is well known that the light intensity regulates the pattern of the tillering (Su et al., 2011). Therefore, I analyzed the contribution of D14 transport to tillering regulation in response to the light intensity.

First, I examined if SL is involved in the light intensity response. WT plants, *d14*,

and *d10-2*, a SL deficient mutant, were grown under a strong light condition or a weak light condition. The tillering was suppressed under a weak light condition compared to that under the strong light condition in WT plants, while the tillering of *d14* and *d10-2* was not influenced by the light intensity (Fig. 2.6 A-D). Next, expression level of genes involved in SL signaling (*D14* and *D3*) or biosynthesis (*D27*, *D17* and *D10*) under the different light intensities was measured. The expression of *D14*, *D3* and *D17* was significantly up-regulated under the weak light condition (Fig. 2.6 E-I). It implies a possibility that the induction of these genes contributes to the suppression of tillering under the weak light condition.

Then, I examined the contribution of D14 transport to the response to light intensity. *d14* mutants containing *pD14::D14:GFP* or *pD14::D14:3xGFP* genes were grown under low or high light intensity and numbers of tillers were measured. As shown in Fig. 2.7, both of these lines were able to respond to the light intensity, and the number of tillers was reduced under weak light. This result suggests that D14 transport is not required for the light intensity response.

2.4. Discussion

Results obtained in this section demonstrate that D14 protein is transported to axillary buds through phloem. To our knowledge, D14 is the first mobile protein which functions in plant hormone signaling.

In this research, the significance of D14 transport for the function of D14 could not be revealed. Grafting experiments using pea, however, showed that the transport of RMS3, a pea D14 ortholog, has potential to regulate shoot branching (Beveridge and

Rameau, personal communication) (Table 1.1). In the grafting experiments in pea, WT rootstock suppressed shoot branching of *rms3* mutant scion (Fig. 2.8). This result indicates that RMS3 or downstream components of the SL signal is transported to the scion. *RMS4*, a pea *D3* ortholog, is another component of SL signaling (Table 1.1). The branching of *rms4* mutant scion was not suppressed by WT rootstock (Fig. 2.8). In contrast, the branching of *rms3* scion was suppressed by the rootstock of *rms4* mutant, in which SL signaling does not occur (Fig. 2.8). These results imply that RMS3 itself, but not downstream components of RMS3, is transported and that transported RMS3 suppresses shoot branching.

Next, I hypothesized that the RMS3 / D14 transport is involved in fine tuning of the shoot branching pattern in response to environmental and / or developmental conditions. As a candidate of environmental signal which controls shoot branching through D14 transport, I tested the light intensity. However, results showed that D14 transport is not required for the light intensity response. There is another possibility that D14 transport is involved in the sensing of light quality rather than light intensity. It has been known that the high ratio of far led light to red light suppresses shoot branching (González-Grandío et al., 2013; Kebrom et al., 2010; Whipple et al., 2011). Thus, red / far red light condition might be another feasible candidate for the environmental signal. Since axillary buds are enclosed in several leaves in many species, it may be difficult for axillary buds to sense the light quality accurately. Plants may be able to overcome this difficulty if *D14* RNA expression and / or D14 protein transport in leaves are regulated by red / far red ratio.

D14 transport might participate in the control of other SL functions. For example, SLs are involved in the control of the root system architecture (Arite et al., 2012;

Kapulnik et al., 2011; Rasmussen et al., 2012; Ruyter-Spira et al., 2011). It is postulated that many kinds of known and unknown macromolecules are transported from shoots to roots through phloem (Turgeon et al., 2009). Because *D14* mRNA is more highly expressed in leaves than in roots, it is appropriate to presume that regulation of root architecture by SLs relies on D14 transported from leaves (Arite et al., 2009; Turgeon et al., 2009). In this case, the rate and amount of D14 transport may be a determinant for the architecture of the root system. These possibilities should be tested in the near future.

Table 2.1. Primers used in Chapter 2

	name	sequence 5' → 3'
construction	D14 F1	CACCGGATCCCCTTGTCTAAGACCTTT
	D14 F2	TCTAGAGGATCCCCTTGTCT
	D14 F3	CACCCCAATCCGCCGCGCTGGTGTG
	D14 R	GTACCGGGCGAGAGCGCG
	GFP F	CCCGGGATGGTGAGCAA
	GFP R1	CCCGGGTTACTTGTACAGCT
	GFP R2	CCCGGGCTTGTACAGCTCGT
	OsHSP F	AAGCTTCCTTCCGGCGATCTTGCAG
	OsHSP R	TCTAGAGCTCCTCCTCTCCTCACACAA
qPCR	D14 RT F9	CATCCGACGACCTGACCTC
	D14 RT R9	CGTGGTAGTCGCTGTCGTTC
	D3 RT F	GGGATGGCGTGTGCAGAT
	D3 RT R	TCAACATGCCCGATAATGACA
	D10 RT F	CGTGGCGATATCGATGGT
	D10 RT R	CGACCTCCTCGAACGTCTT
	D17 RT F	GATGGTGGCTATGTTCTTCTTGTA
	D17 RT R	TGCATTCTCTGTCCCTATCTTCT
	D27 RT F	TCTGGGCTAAAGAATGAAAAGGA
	D27 RT R	AGAGCTTGGGTCACAATCTCG
	UBQ RT F	AGAAGGAGTCCACCCTCCACC
	UBQ RT R	GCATCCAGCACAGTAAAACACG

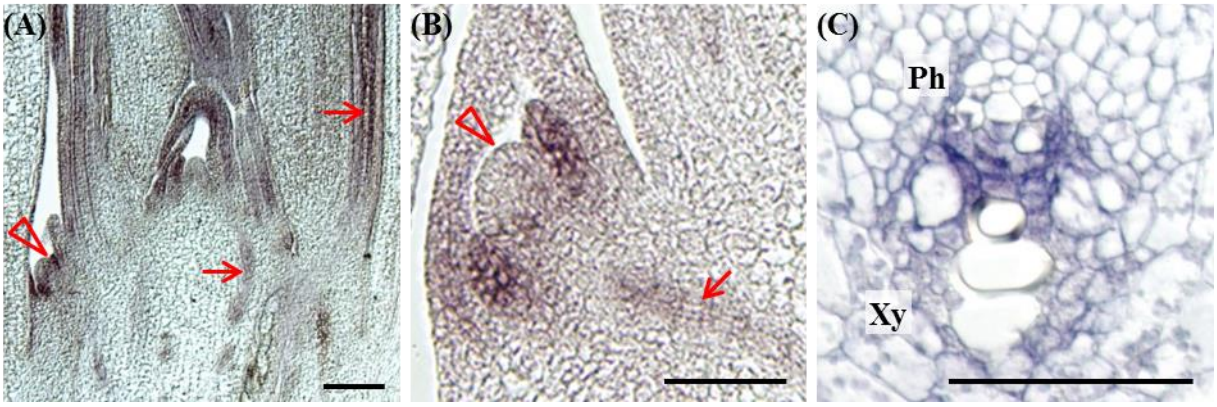

Figure 2.1. *D14* mRNA expression pattern.

in situ hybridization using *D14* mRNA anti-sense probe. (A) A longitudinal section of a young rice plant. (B) Axillary bud. (C) Vascular bundle of mature leaf sheath. *D14* mRNA is expressed in sieve element, xylem parenchyma of vascular bundles, leaf primordia, and young leaves. Arrows: vascular bundles. Triangles: Axillary meristems. ; Ph, phloem; Xy, xylem; Bars: 50 μm.

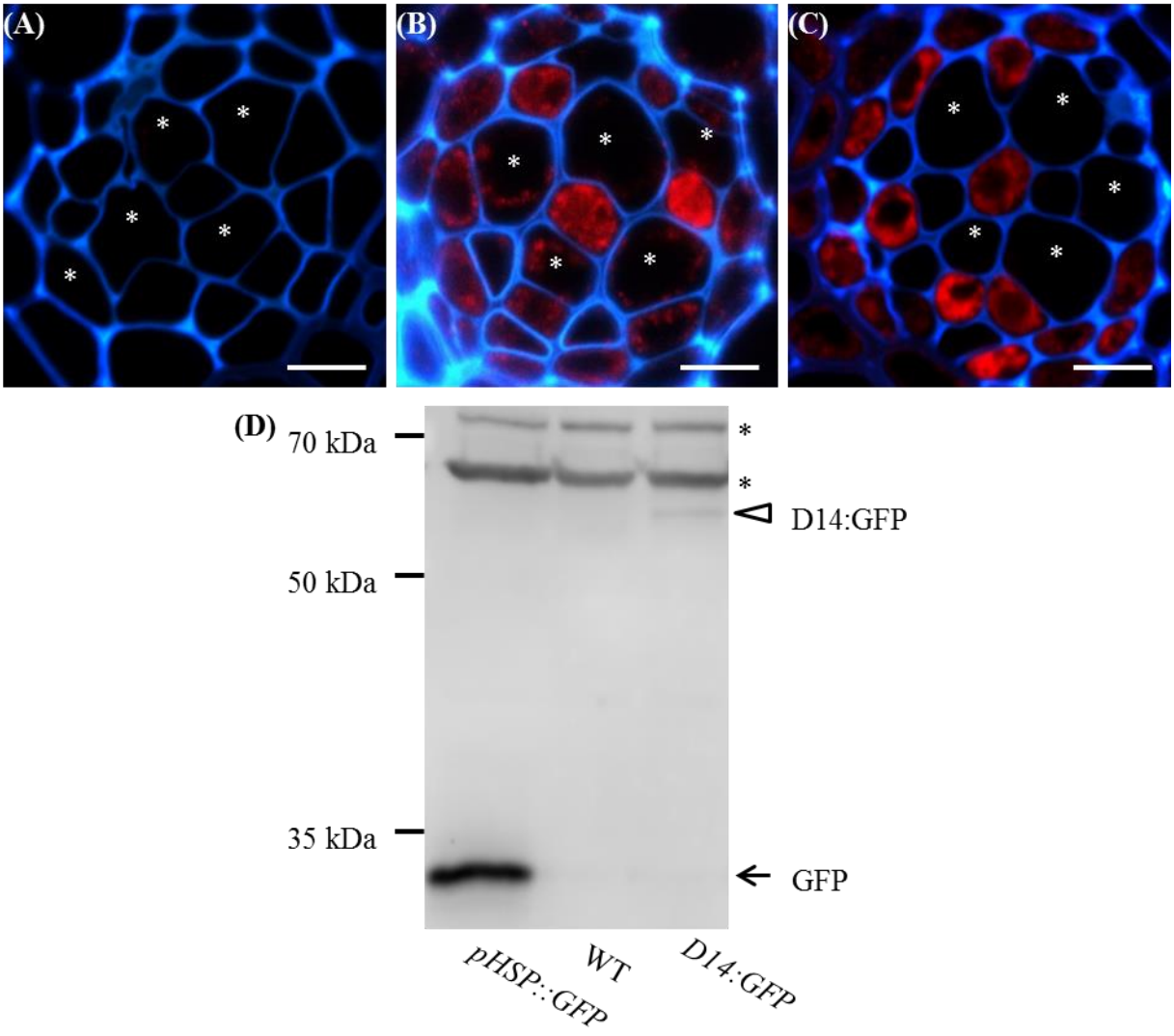

Figure 2.2. D14 protein is distributed in sieve element

Immune staining of phloem using anti-GFP antibody. (A) WT. (B) *pD14::D14:GFP.* (C) *pD14::D14:3xGFP.* D14:GFP is present in sieve elements, while D14:3xGFP is not detected. Red signal indicates D14:GFP or D14:3xGFP protein. Blue signal corresponds to cell wall ultraviolet auto-fluorescence from cell wall. Asterisk: sieve elements. Bars: 5 μm. (D) Western blotting analysis of extracts from *pD14::D14:GFP* lines with anti-GFP antibody. *pHSP::GFP* and WT were used as controls. Arrow: GFP. Triangle: D14:GFP. Asterisks: nonspecific band.

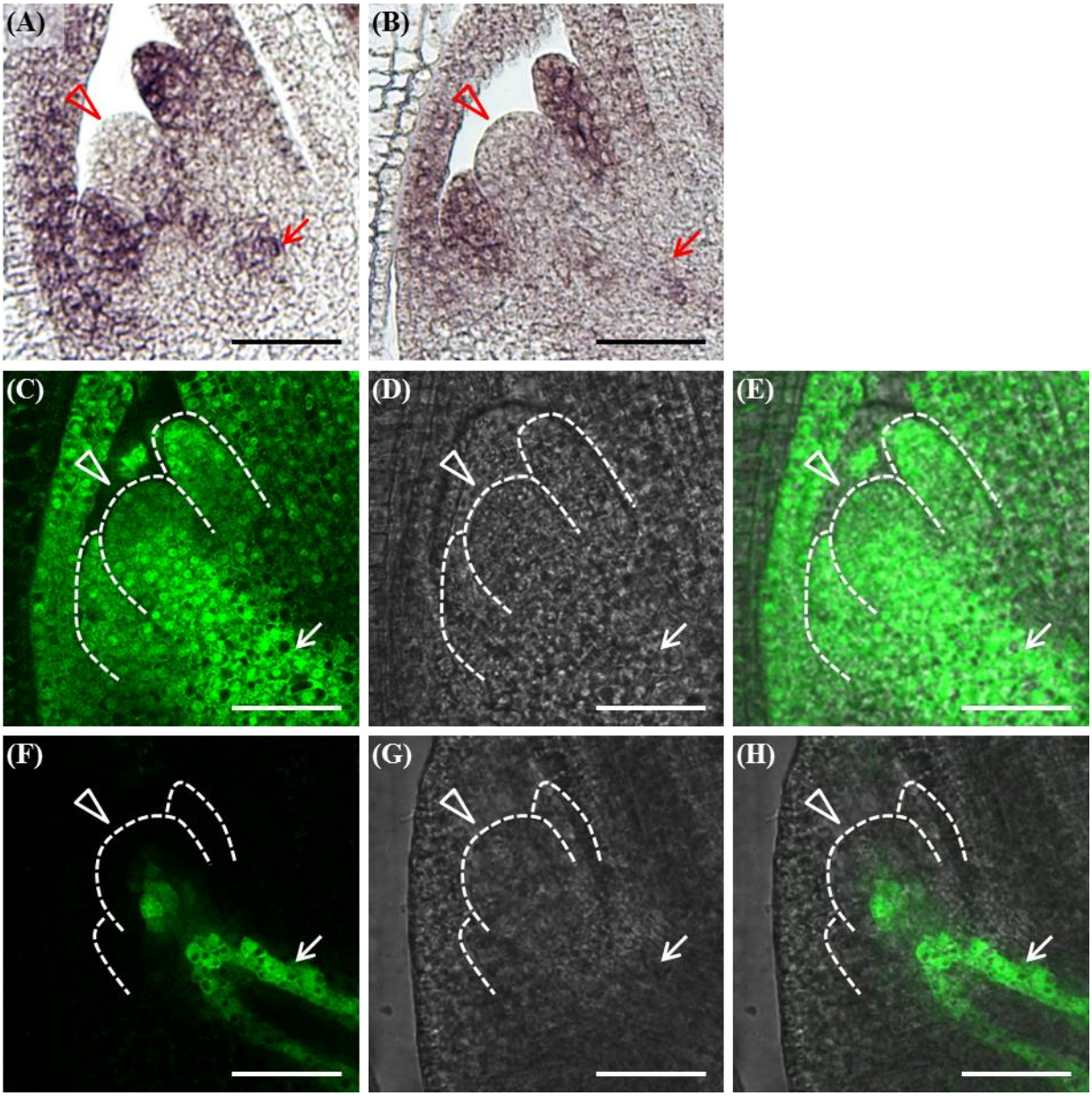

Figure 2.3. D14 protein is transported to axillary buds.

Axillary buds of *pD14::D14:GFP* (A, C-E) and *pD14::D14:3xGFP* (B, F-H). (A, B) *in situ* hybridization with *GFP* antisense probe in *pD14::D14:GFP* (A), and in *pD14::D14:3xGFP* (B). The signal patterns of these lines were indistinguishable from that of endogenous *D14* mRNA. (C,F) GFP fluorescence. (D,G) visible light. (E, H) merge. D14:GFP is transported to axillary buds, while D14:3xGFP is not. Arrows: vascular bundles. Triangles: Axillary meristems. Bars: 50 μm.

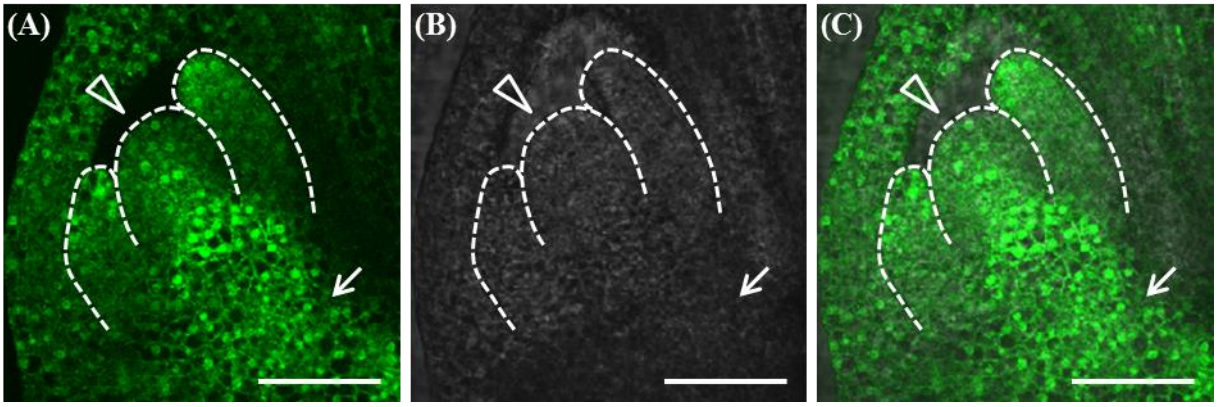

Figure 2.4. SLs are not required for D14 transport.

GFP florescence in axillary buds of *pD14::D14:GFP* in *d10* background. (A) GFP fluorescence. (B) visible light. (C) marge. D14:GFP is transported to axillary buds, in spite that concentration of SLs are below a detectable level. Arrows: vascular bundles. Triangles: Axillary meristems. Bars: 50 μm.

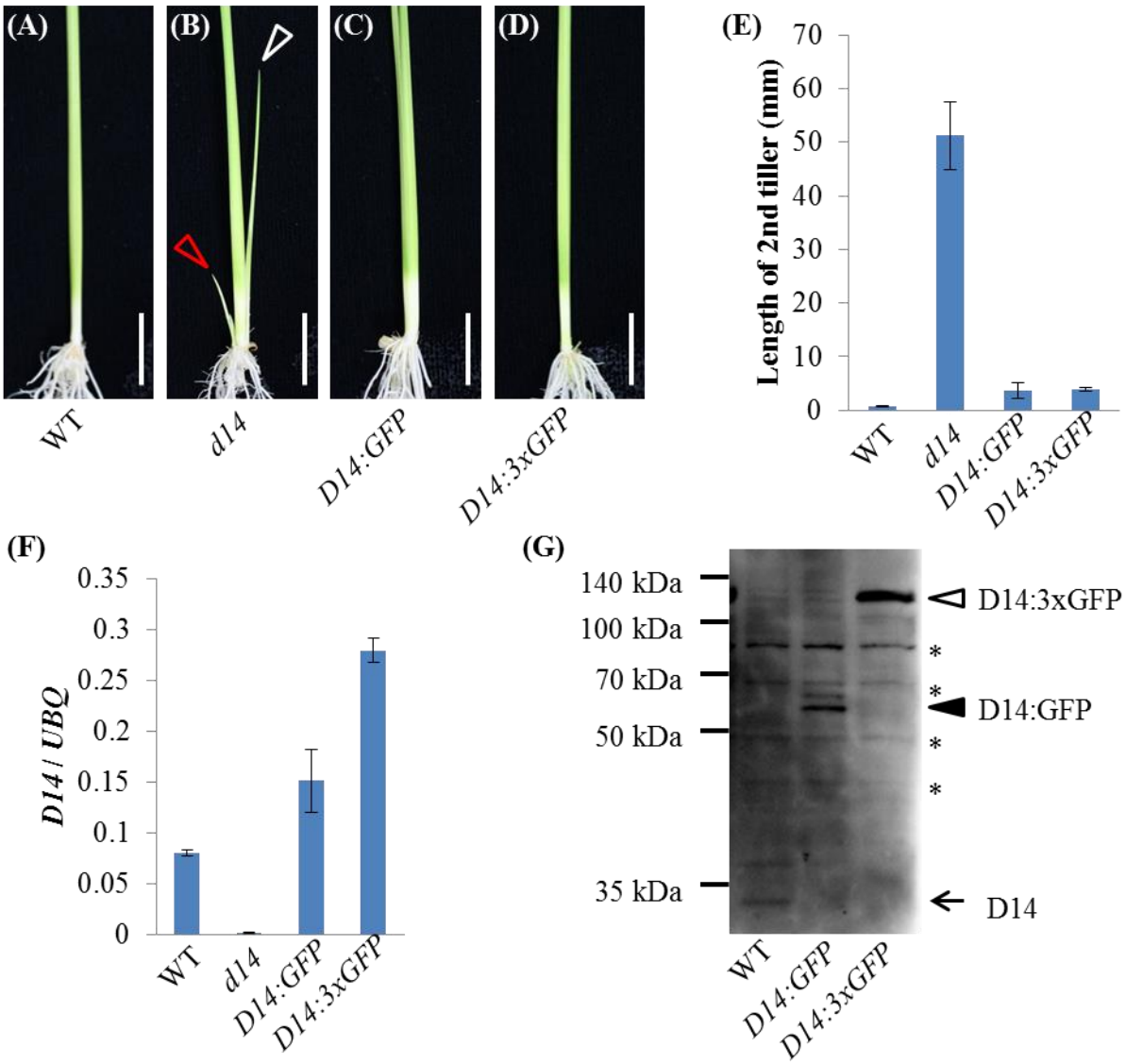

Figure 2.5. D14 transport is not essential to *D14* function

(A-D) Tillering phenotype of WT (A), *d14* (B), *pD14::D14:GFP* (C), and *pD14::D14:3xGFP* (D). The tillers in the axils of the first (red) and the second (white) leaves grew only in *d14*, but not in *pD14::D14:GFP, pD14::D14:3xGFP* lines. Bars: 10 mm (E) Length of the tillers in the axils of the second leaves. Data are means ± standard error. n = 6–10. (F) Expression level of *D14* mRNA. Data are means ± standard error. n = 3. (G) Western blotting analysis of extracts from *pD14::D14:GFP* and *pD14::D14:3xGFP* lines with anti-D14 antibody. Arrow: D14. Black triangle: D14:GFP. White triangle: D14:3xGFP. Asterisks: nonspecific band.

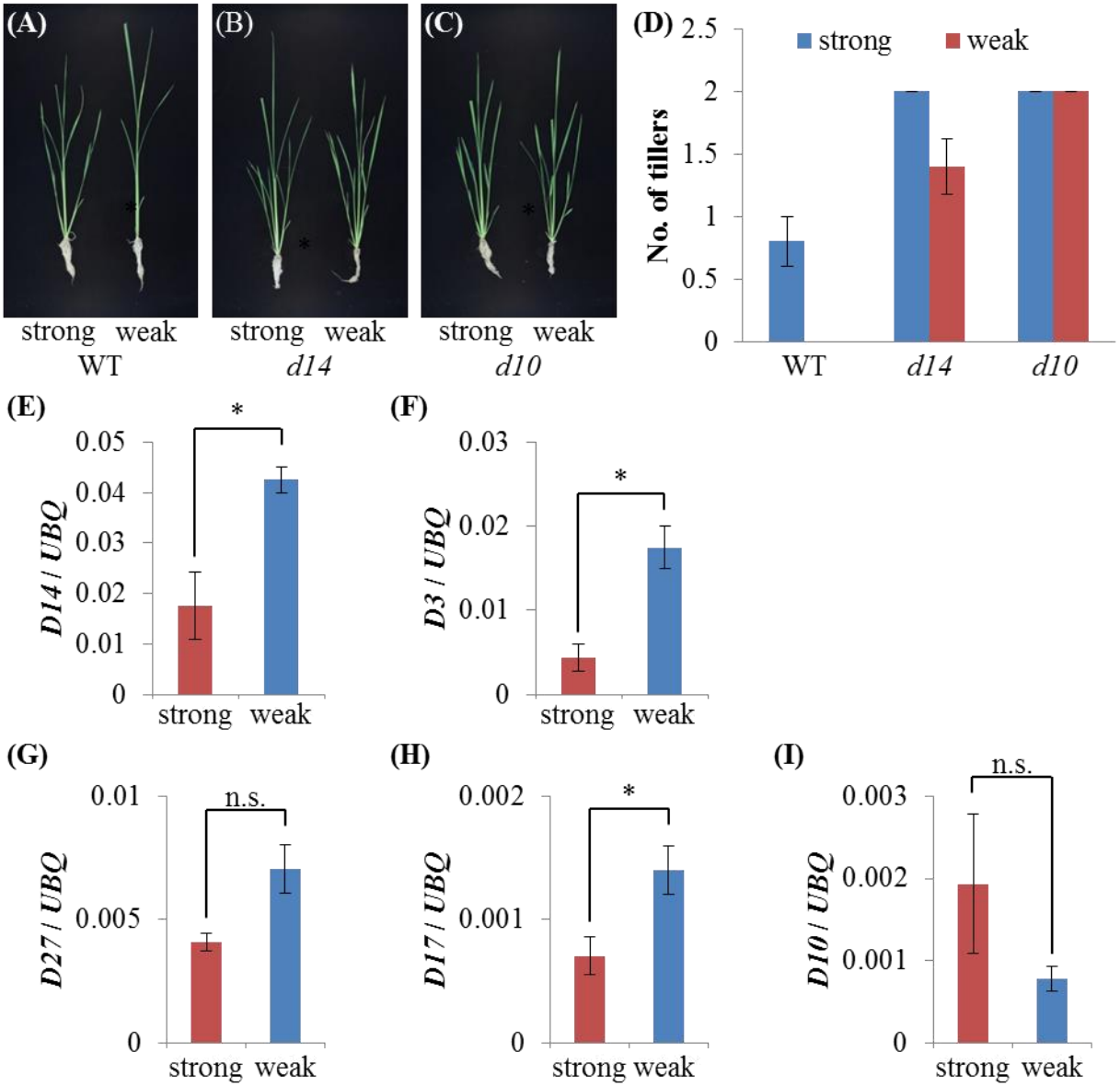

Figure 2.6. SLs regulate tillering in response to light intensity.

(A-C) Growth of WT plants (A), *d14* mutants (B) and *d10-2* mutants under high and low light intensities. (D) The numbers of tillers of 5th leaf stage WT, *d14*, and *d10-2*. Tillering of WT was suppressed under weak light condition, while that of SL mutants was not. Data are means ± standard error. n = 10. (E-I) The expression level of SL signaling or biosynthesis genes in response to light amount. *D14* (E) and *D3* (F) work in SL signaling pathway, and *D27* (G), *D17* (H), and *D10* (I) work in SL biosinthesis pathway. *D14*, *D3*, and *D17* were induced under weak light conditions. Data are means ± standard error. n = 3. * $P < 0.05$; n.s., not significance (*t* test).

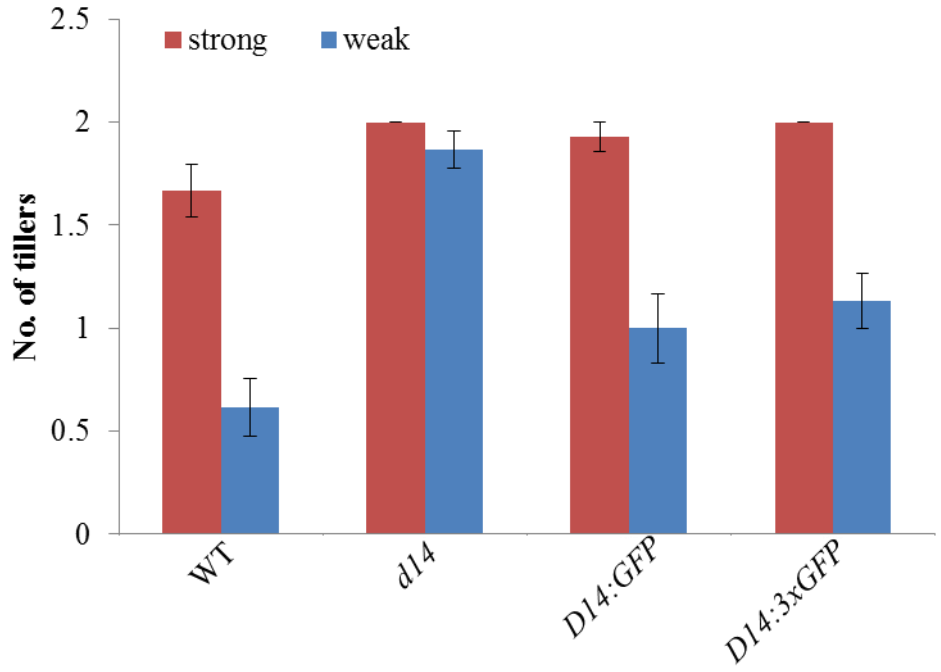

Figure 2.7. SLs regulate tillering in response to light amount

The numbers of tillers of 5th leaf stage WT, *d14*, *pD14::D14:GFP* lines, and *pD14::D14:3xGFP* lines under strong and weak light conditions. Both *pD14::D14:GFP* and *pD14::D14:3xGFP* lines were able to response to light amount. Data are means ± standard error. n = 13-15.

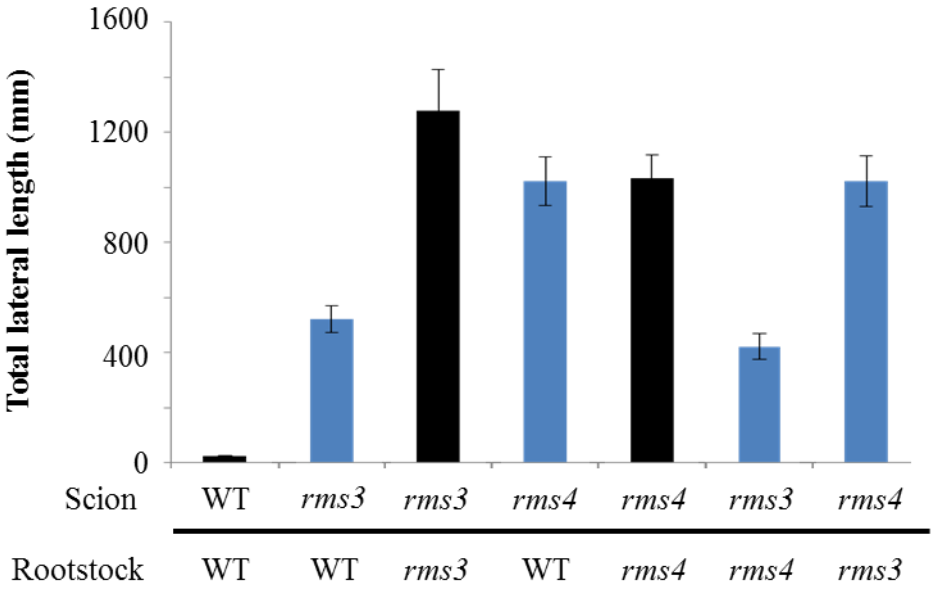

Figure 2.8. Grafting between WT and *rms* mutants.

Total length of shoot branches of scions. The shoot branching of *rms3* mutant scions was suppressed by WT and *rms4* mutant rootstocks. On the other hand, the shoot branching of *rms4* mutant scions was not suppressed by WT rootstocks. Data are means ・ standard error. These data were obtained by Dr. Elizabeth Dun and Prof. Christine Beveridge.

3. *DWARF14 LIKE* of rice suppresses mesocotyl elongation *via* a strigolactone independent pathway under dark conditions

3.1. Introduction

It has been shown that *MAX2*, the Arabidopsis *D3* ortholog, functions in the SL signaling pathway (Gomez-Roldan et al., 2008; Umehara et al., 2008) (Table 1.1). In addition, *MAX2* is involved in photomorphogenesis (Nelson et al., 2011; Shen et al., 2007; Shen et al., 2012; Stirnberg et al., 2002). *max2* mutants are hyposensitive to light, while *Atd14* mutant and SL deficient mutants do not exhibit any abnormalities in photomorphogenesis (Nelson et al., 2011; Shen et al., 2007; Shen et al., 2012; Stirnberg et al., 2002; Waters et al., 2012). It suggests that *MAX2* regulates photomorphogenesis *via* an SL independent pathway. Recent findings indicate that *KAI2*, the Arabidopsis *D14L* ortholog, cooperate with *MAX2* in regulating photomorphogenesis (Table 1.1). *kai2* shows light-hyposensitive phenotypes as observed in *max2* (Nelson et al., 2011; Sun et al., 2010; Waters et al., 2012). *max2* and *kai2* were insensitive to karrikins, chemicals which enhance seed germination and photomorphogenesis, indicating that both *MAX2* and *KAI2* function in karrikin signaling (Nelson et al., 2011; Sun et al., 2010; Waters et al., 2012) (Fig. 3.1 A). While *max2* works in both SL and karrikin signaling pathways, it has been shown that *KAI2* is not involved in SL signaling (Scaffidi et al., 2014).

In contrast to the situation in Arabidopsis, SL deficient or insensitive mutants show phenotypes in skotomorphogenesis in rice. The mesocotyls of SL deficient and insensitive mutants of rice are longer than those of WT plants under dark conditions (Hu

et al., 2010; Hu et al., 2014). *d3* mutants exhibit significantly stronger phenotypes than the other mutants, indicating that *D3* has extra functions in addition to the SL signaling (Hu et al., 2010; Hu et al., 2014). The function of *D14L* in rice was unknown.

In this chapter, In order to reveal the functions of *D14L* clade genes and the specification of functions among *D14* family genes, I analyzed the functions of *D14L* in skotomorphogenesis in rice. I show that *D14L* suppresses mesocotyl elongation under dark conditions *via* an SL independent pathway.

3.2. Materials and methods

Plant materials and growth conditions

d3-1, *d3-2*, and *d14-1* were described previously (Arite et al., 2009; Ishikawa et al., 2005; Yoshida et al., 2012).

To observe the mesocotyl phenotypes seeds were sterilized in 2.5% (v/v) sodium hypochlorite and grown on 0.7% (w/v) agar in a growth chamber at 28° C under dark condition or in continuous light. Plants grown in a glasshouse (13h light at 28° C, 11h dark at 24° C) were used to analyze the tiller number, plant height, and sub-cellular localization of D14L protein.

Plasmid construction and transgenic rice production

To construct *D14L* RNAi vector, a partial cDNA of *D14 LIKE* containing a portion of the open reading frame and 3'-untranslated region was amplified using a primer set,

D14L RNAi F and *D14L* RNAi R. The PCR fragment was cloned into pENTR/D-TOPO (Life Technologies). The fragment was transferred into pANDA by recombination reaction (Miki & Shimamoto, 2004; Miki et al., 2005) using LR clonase (Life Technologies) according to the manufacturer's instructions. To construct *p35S::D14L:GFP* vector, the *D14L* ORF was amplified using a primer set, *D14L* F and *D14L* R. The PCR fragment was cloned into pENTR/D-TOPO, and the fragment was transferred into pGWB5 (Nakagawa et al., 2007) using LR clonase. *D14L* RNAi vector was transformed into WT plants (cv Nipponbare) and the *d14-1* mutant (cv Shiokari), and *p35S::D14L:GFP* vector was transformed into WT rice (cv. Nipponbare) as described by Nakagawa et al. (2002). Primer sets used for construction were described in Table 3.1.

SL treatment

For SL treatments, 1 μM synthetic SL analog, (rac)-GR24 (Chiralix), was added to the agar plate (Hu et al., 2010).

Quantitative reverse transcription-PCR

Total RNA was extracted from shoots of 7 day old seedlings using Plant RNA Isolation kit (Agilent Technologies). After DNase I treatment, first-strand cDNA was synthesized using SuperScript III reverse transcriptase (Life Technologies). PCR was performed with SYBR green using Light Cycler 480 System II (Roche Applied Science, Penzberg, Germany). Primer sets used for qPCR were described in Table 3.1.

In situ hybridizations

In situ hybridizations were performed using 7 day old seedlings as described by Kouchi et al. (1995). The full length *D14L* cDNA was amplified using a primer set *D14L* F and *D14L* R. The PCR fragment was cloned into pBluescript SK and used as a template to make antisense and sense probes.

Subcellular localization of the D14L protein

Expanding leaf blades collected from plants grown in a greenhouse were used. GFP fluorescence was observed using a confocal microscope (OLYMPUS FV1000).

3.3. Results

3.3.1. *D14L* does not regulate shoot branching and plant height.

To examine the role of *D14L*, I introduced *D14L* RNAi construct into WT plants and *d14-1* mutant. Independent 43 lines were generated in WT background, and two lines (line 8 and 43) in which the expression of *D14L* was strongly suppressed were chosen for analysis (Fig. 3.2 A). In these lines, the expression of *D14* was not reduced (Fig. 3.2 B). In *d14-1* background, one line, in which the expression level of *D14L* was significantly low, was used (Fig. 3.2. C).

First, I analyzed if *D14L* regulates tillering and plant height as *D14* does (Ishikawa

et al., 2005). Numbers of tillers and plant height of *D14* RNAi lines in WT background were not significantly different from those of WT (Fig3.3 A, C). In addition, reduction of *D14L* expression did not affect the number of tillers and the plant height in *d14-1* background. These results demonstrate that *D14L* does not function in the control of tillering and plant height regulation.

3.3.2. *D14L* suppresses mesocotyl elongation under dark conditions

To examine the role of *D14L* in mesocotyl growth, I measured mesocotyl elongation in *D14L* RNAi lines in WT background. Seeds of WT plants, the *D14L* RNAi lines, and the *d3-2* mutant were germinated and grown on agar plates for 8 days. No difference was observed between WT, *D14L* RNAi lines and *d3-2* mutant in light (Fig. 3.4). In contrast, under dark conditions, the mesocotyls of the *D14L* RNAi lines were longer than those of WT ($P < 0.05$, *t* test) (Fig. 3.5 B). This indicates that *D14L* functions to suppress mesocotyl elongation in the dark. It was reported that the mesocotyls of *d3* mutants are significantly longer than those of *d14* and other SL related mutants (Hu et al., 2010). The mesocotyls of *d3-2* mutants were also longer than those of the *D14L* RNAi lines ($P < 0.001$, *t* test) (Fig. 3.5 B).

3.3.3. *D14* and *D14L* function in an additive manner

Previous report and my result showed that both *D14* and *D14L* suppress mesocotyl elongation in dark (Hu et al., 2010; Hu et al., 2014) (Fig 3.5 B). Next, I compared the phenotypes of *d14-1* mutants and *D14L* RNAi *d14-1*plants to uncover the relationship

between *D14* and *D14L* in the control of mesocotyl growth. The mesocotyls of the *D14L* RNAi *d14-1* plants were significantly longer than those of the *d14-1* single mutants ($P < 0.05$, *t* test) (Fig. 3.5 C). This result indicates that *D14* and *D14L* work additively to suppress mesocotyl elongation.

3.3.4. *D14L* functions *via* an SL independent pathway

In order to clarify whether *D14L* functions in the SL signaling pathway to suppress mesocotyl elongation, I examined the effect of synthetic SL analog treatment on the mesocotyl phenotype. Seedlings were grown on agar plates containing a 1 μM racemic mixture of GR24 and the mesocotyl length was measured (Fig. 3.1 B). As described in previous reports, mesocotyl elongation of WT seedlings is suppressed by the application of GR24, whereas *d14* and *d3* mutants did not response to the addition of GR24 (Hu et al., 2010; Hu et al., 2014) (Fig. 3.5). In the *D14L* RNAi lines, mesocotyl elongation was significantly suppressed by the application of GR24 ($P < 0.01$, *t* test) (Fig 3.5 B). One the other hand, the *D14L* RNAi *d14-1* plants did not respond to GR24 treatment (Fig. 3.5 C). Taken together, these results showed that both *D14* and *D14L* act to suppress mesocotyl elongation; however, *D14* functions in the SL signaling pathway while *D14L* functions in an as yet unknown SL independent pathway.

3.3.5. Regulation of *D14L* mRNA expression

I showed that *D14L* RNAi lines exhibited the elongated mesocotyl phenotype only under dark conditions in rice (Fig. 3.4, Fig. 3.5). In Arabidopsis, it was shown that the

KAI2 (the ortholog of rice *D14L*) mRNA expression is suppressed under dark conditions and that *kai2* mutants exhibit the elongated hypocotyl phenotype only in light condition in Arabidopsis (Sun et al., 2010). Therefore, I analyzed if *D14L* mRNA expression is regulated by light. WT plants were grown for 4 days in light or under dark condition, and *D14L* mRNA expression in the shoots was measured. There was no significant difference in the expression levels of *D14L* mRNA between dark-grown and light-grown shoots (Fig. 3.6 A).

In order to determine the spatial localization of *D14L* expression, I carried out *in situ* hybridization experiments. Results show that *D14L* mRNA is expressed in the vascular bundles and the crown root primordia (Fig. 3.6 B-F).

3.3.6. Sub-cellular localization of D14L protein

In Arabidopsis, KAI2 protein is present in the nucleus and the cytosol (Zhou et al., 2013). To determine the subcellular location of the D14L protein, I produced transgenic rice plants expressing D14-GFP fusion protein under the control of the CaMV 35S promoter. GFP fluorescence was observed in the nucleus and the cytosol (Fig. 3.7).

3.4. Discussion

In this chapter, I showed that *D14L* suppresses mesocotyl elongation under dark conditions. It was previously reported that *D14* and *D3* also regulate mesocotyl elongation in the dark (Hu et al., 2010). The additive phenotype observed in *d14-1* mutants expressing the *D14L* RNAi construct indicated that *D14* and *D14L* function in

independent pathways. In Arabidopsis two signaling pathways, the SL signaling pathway mediated by *D14* and the Karrikin signaling pathway mediated by *KAI2*, depend on the function of *D3* (*MAX2*) (Arite et al., 2009; Waters et al., 2012). Therefore, an intriguing possibility is that rice *D3* functions in the two signaling pathways mediated by *D14* and *D14L*. This might explain why *d3* mutants show more striking phenotypes than the *d14* mutants or the *D14L* RNAi lines. In Arabidopsis, the phenotype of the *Atd14 kai2* double mutant is similar to that of *max2*. In contrast, the mesocotyls of *d3-1* mutants are much longer than those of the *D14L* RNAi *d14-1* line. A possible explanation for this difference is that other gene(s) are involved in the control of mesocotyl elongation through *D3* in rice. Feasible candidates for such genes are *D14L2a* and *D14L2b* (Waters et al., 2012). In Arabidopsis, *dlk2* mutant shows no visible phenotype (Waters et al., 2012). The possibility that *D14L2a* and *D14L2b* also function in skotomorphogenesis in rice should be tested in the near future. On the other hand, I cannot rule out the possibility that a residual expression of *D14L* mRNA in the RNAi lines hampered the correct evaluation of the phenotypes.

I showed that the *D14L* RNAi lines respond to 1 μM GR24 whereas this response was not observed in the *d14-1* mutants. This indicates that *D14L* is not required for SL signaling. Recent study proposed that *KAI2* does not function in the SL signaling and that *Atd14* mutant is sensitive to racemic mixture of GR24 because of unnatural stereoisomers of GR24 (Scaffidi et al., 2014) (Fig. 3.1 B). In rice, the elongation of *d14-1* mesocotyls was not significantly suppressed by the application of a 1 μM racemic mixture of GR24. It is possible that a higher concentration of GR24 might produce a response in *d14-1* plants, but the most likely explanation is that the SL signal is mediated by *D14* but not by *D14L* (Fig. 3.8).

My results and the previous reports about the functions of *KAI2* may imply that the roles of *D14* and *D14L* are largely conserved in angiosperms. Interestingly, genes in the *D14* clade are not found in mosses, liverworts, and charophytes, even though some of these plants synthesize SLs and are sensitive to SLs (Delaux et al. 2012). It is not yet known whether genes in the *D14L* clade are recruited to mediate SL signaling in these organisms. Furthermore, since *D14L* works in an SL independent pathway in angiosperms and karrikin has not been identified as an endogenous compound, it is possible that *D14L* mediates signals that are as yet unknown. To answer these questions it will be important to further elucidate the functions of *D14L*.

Table 3.1. Primers used in Chapter 3

	name	sequence 5' → 3'
construction	D14L RNAi F	CACCACATAGTCATCCCTGT
	D14L RNAi R	CATAAAACAGAGTTGCAGCTCG
	D14L F	CACCATGGGGATCGTGGAGGAG
	D14L R	GACCGCAATGTCATGCTGGAT
qPCR	D14 RT F3	GGACACGCATCCCTCTACTG
	D14 RT R3	GGACACGCATCCCTCTACTG
	D14L RT F	TGGAGGATTTGAGCAGGAG
	D14L RT R	CACCAGGCCTTGTAGTTTGAC
	UBQ RT F	AGAAGGAGTCCACCCTCCACC
	UBQ RT R	GCATCCAGCACAGTAAAACACG

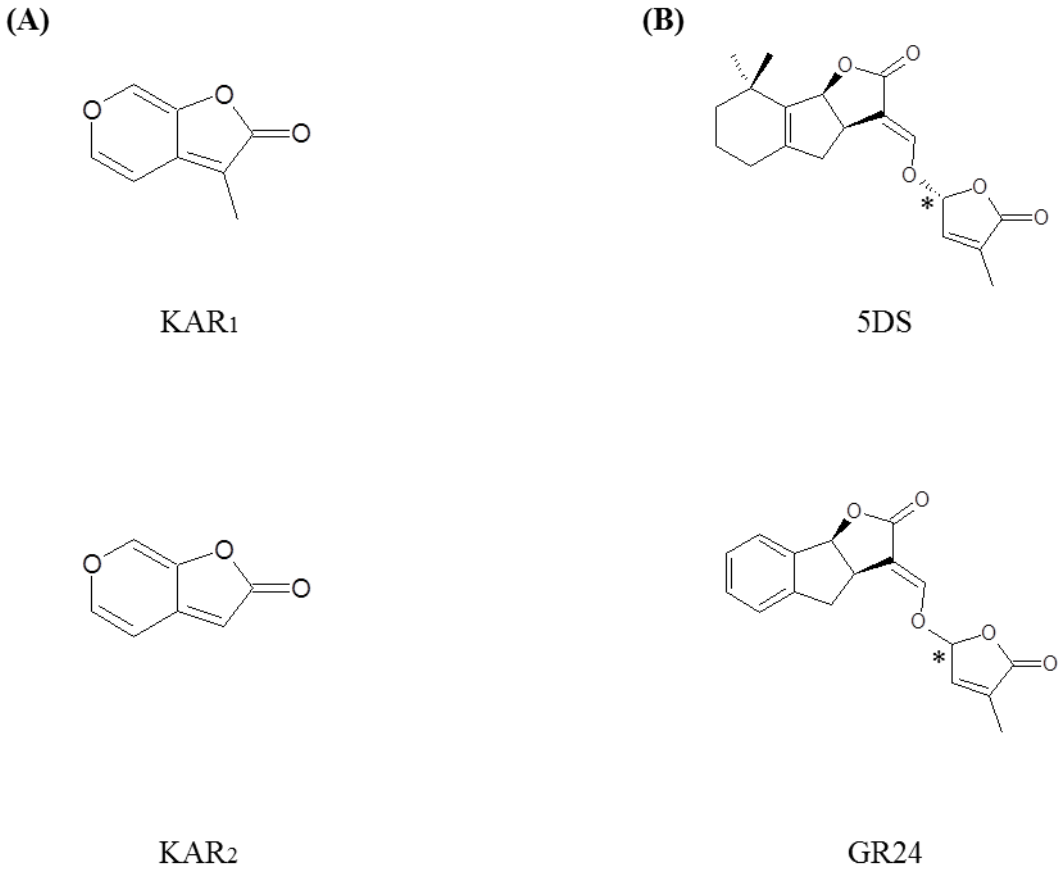

Figure3.1. Structures of karrikins and SLs

(A) Structures of highly active karrikins, KAR1 and KAR2. (B) Structures of one of major natural SLs in rice, 5DS, and synthetic SL analog, GR24. All natural SLs have C2' R configuration (marked with *), while GR24 used in this study was racemic mixture of two configuration.

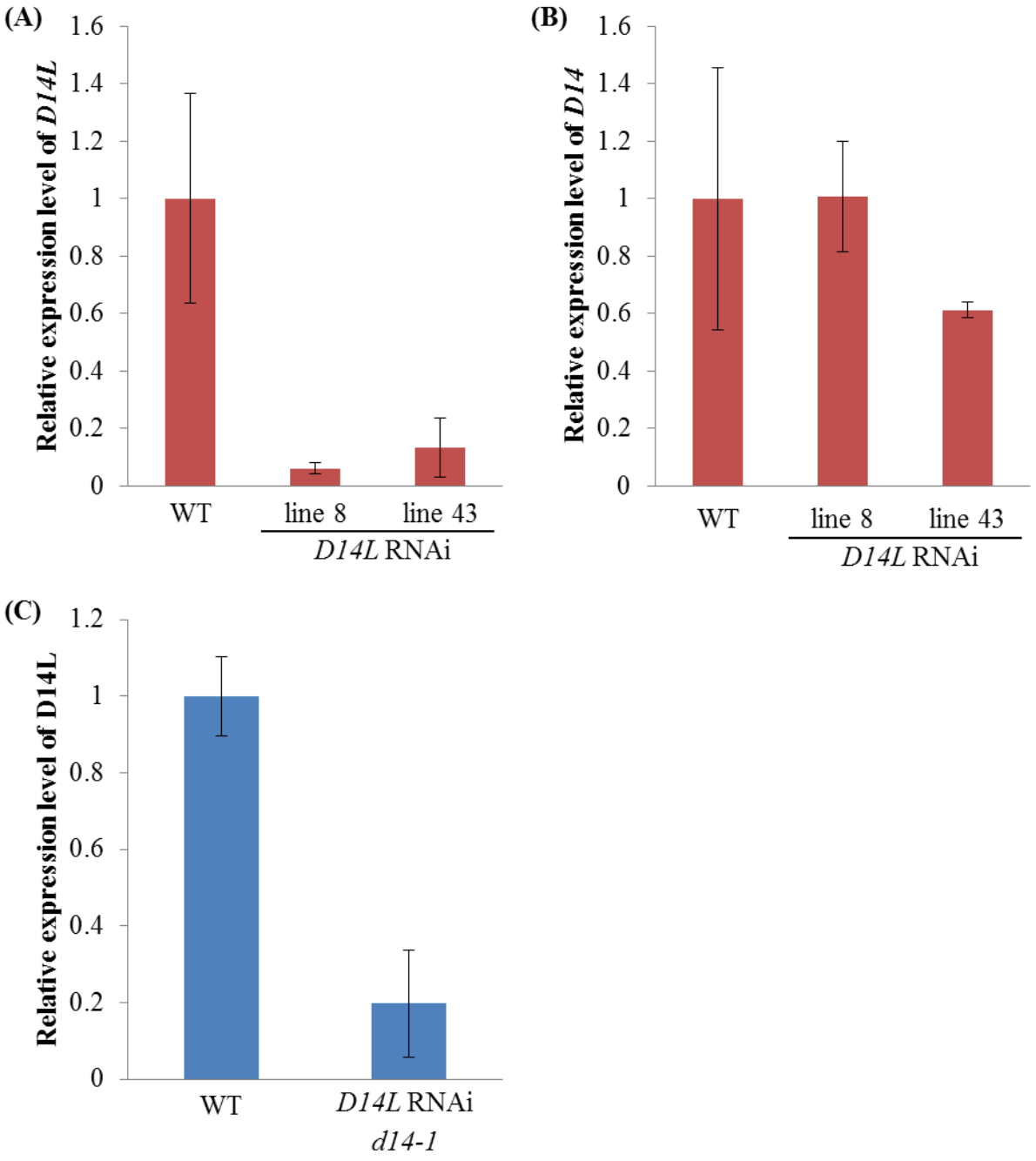

Figure 3.2. Relative expression level of *D14L* and *D14* in *D14L* RNAi lines.
Expression levels of *D14L* and *D14* were measured in 8 day old seedling shoot. (A) Relative expression level of *D14L* in *D14L* RNA lines In the WT background. (B) Relative expression level of *D14* in *D14L* RNA lines in WT background. (C) Relative expression level of *D14L* in *D14L* RNA lines in *d14-1* background. Data are means ± standard error. n = 2-3 biological replicates, 3 plants / sample.

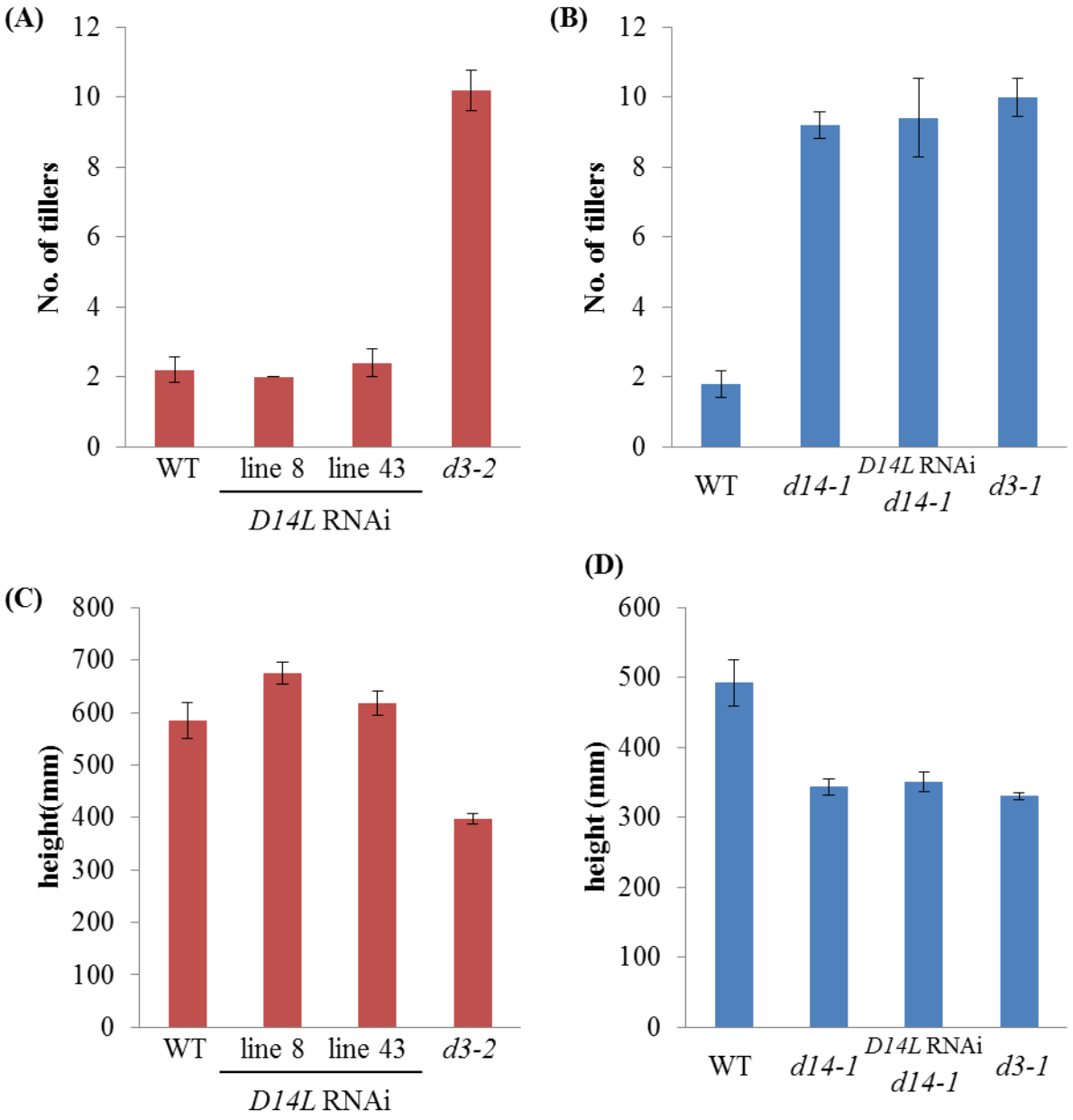

Figure 3.3. Shoot branching and plant height phenotypes of *D14L* RNAi lines

(A, B) Numbers of tillers of 9th leaf stage plants in Nipponbare background (A) and Shiokari background (B). (C, D) Plant height of 9th leaf stage plants in Nipponbare background (C) and Shiokari background (C). Data are means ± standard error. n = 5.

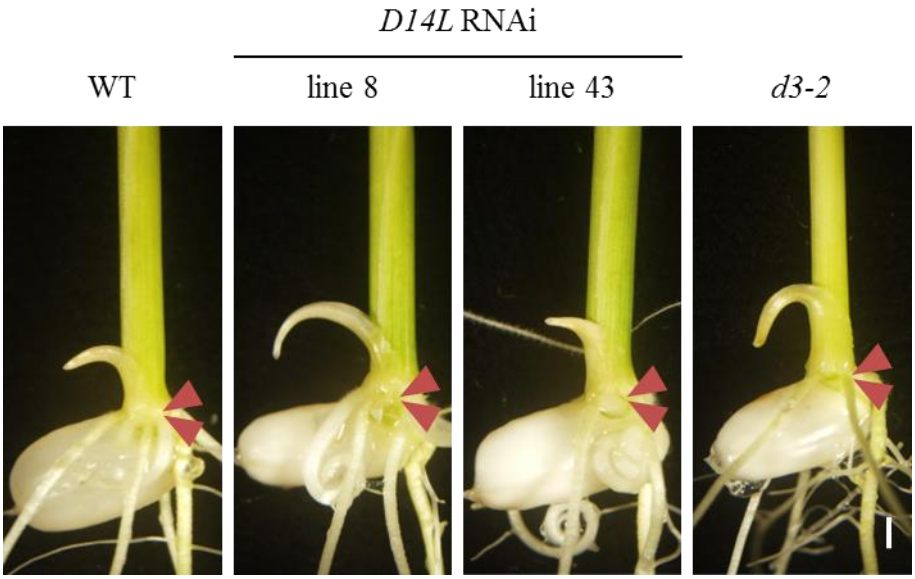

Figure 3.4. Mesocotyl phenotypes of *D14L* RNAi lines in light.
Morphology of mesocotyls of 8 day old seedlings grown in light. Arrows indicate mesocotyls. Bar = 1 mm.

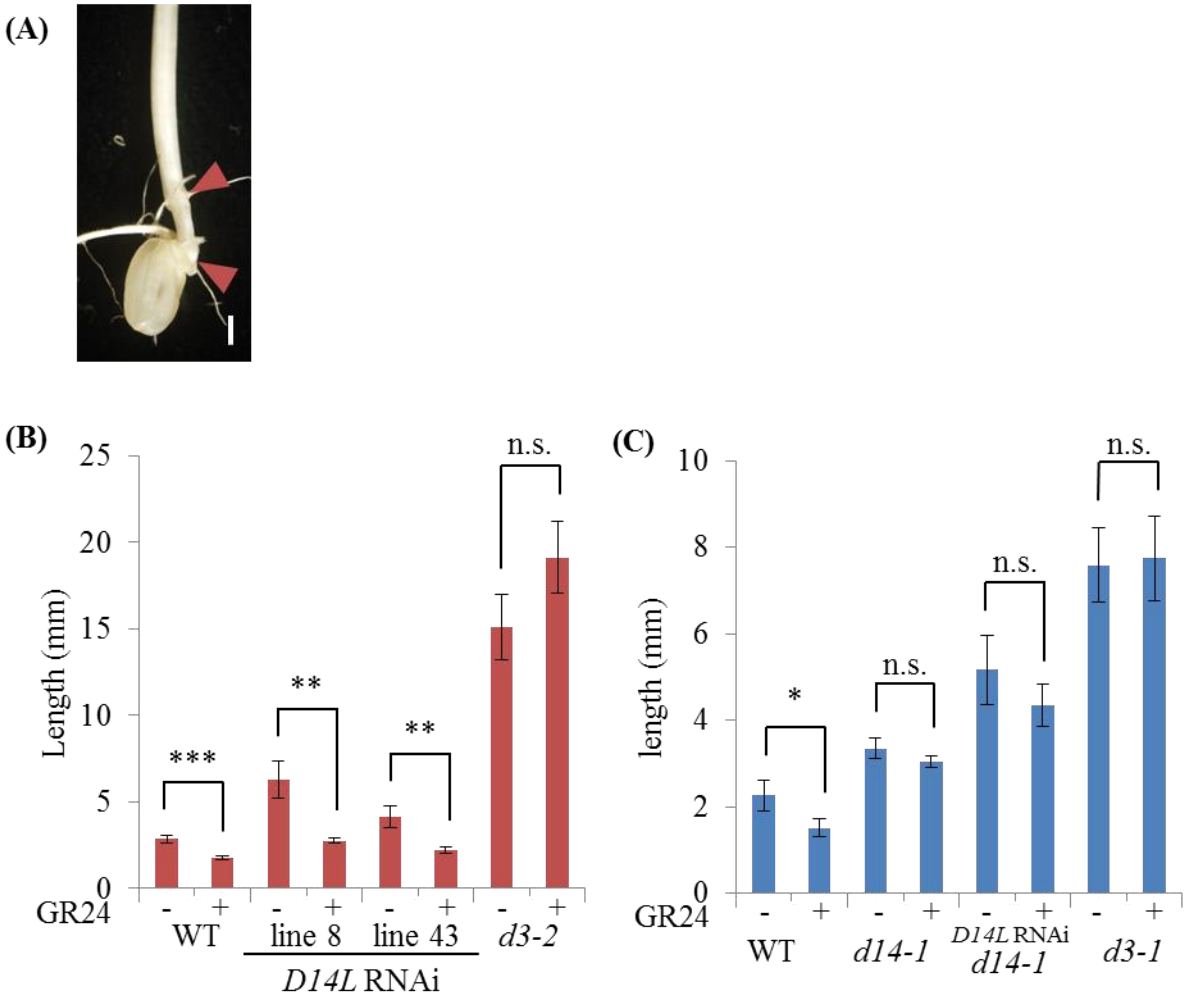

Figure 3.5. Mesocotyl phenotypes of *D14L* RNAi lines under dark conditions.

(A) The mesocotyl of 8 day old WT plants under dark conditions. Arrows indicate the top and the bottom parts of the mesocotyl. Bar = 1 mm. (B) Lengths of mesocotyls of the Nipponbare background plants under dark conditions. (C) Lengths of mesocotyls of the Shiokari background plants under dark conditions. *** $P < 0.001$; ** $P < 0.01$; * $P < 0.05$; n.s., not significance (*t* test). Data are means ・ standard error. n = 9–44. All data for (B) and (C) are provided in Supplemental Table.

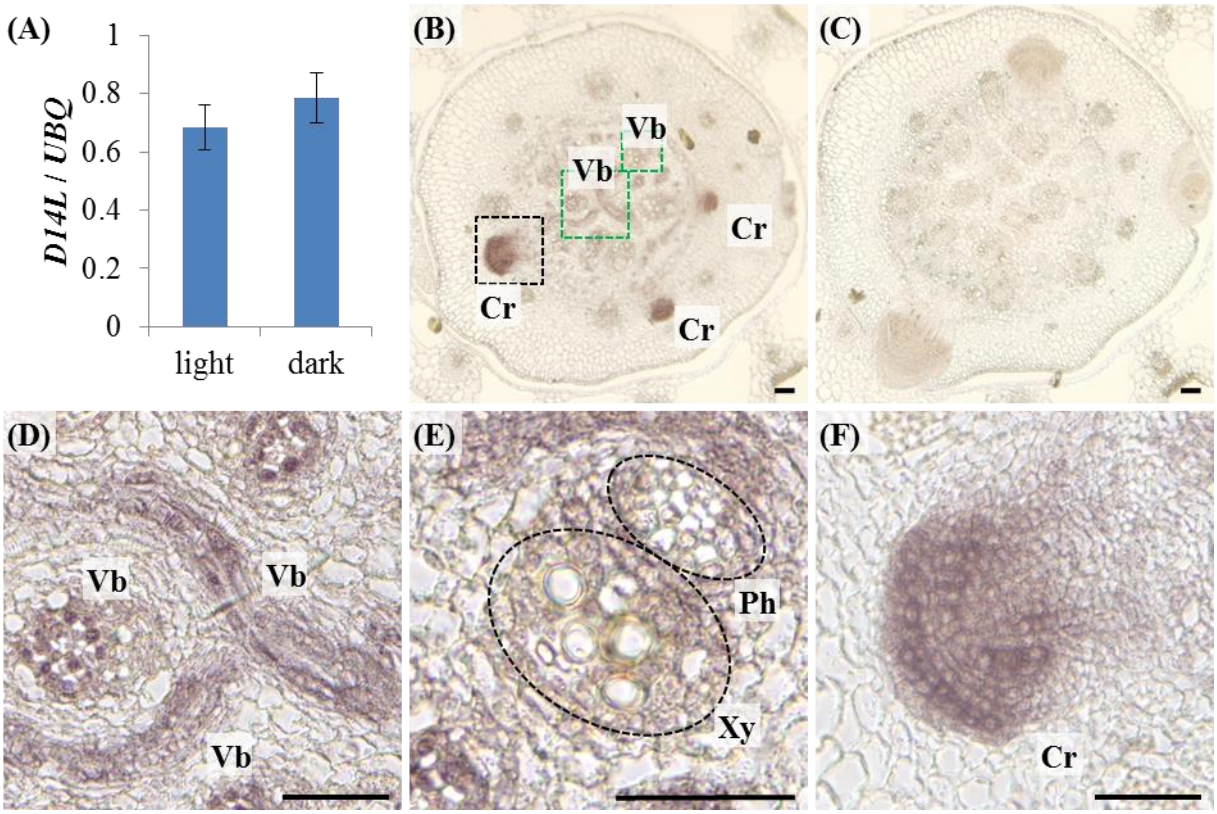

Figure 3.6. Regulation of *D14L* mRNA expression.

(A) Expression level of *D14L* in shoots of 4 day old WT seedlings grown in light or under dark condition. Data are means ・ standard error. n = 3 biological replicates, 3 plants / sample. (B) Cross section of the internode hybridized with *D14L* mRNA anti-sense probe. The enlarged views of the vascular bundles (green square), and the crown root primordia (brack square) are shown in (D), (E), and (F). (C) Cross section of the internode hybridized with *D14L* mRNA sense probe. (D, E) vascular bundles. (F) Crown root primordia. Vb, Vascular bundle; Cr, Crown root primordia; Ph, phloem; Xy, xylem; bar = 50 μm.

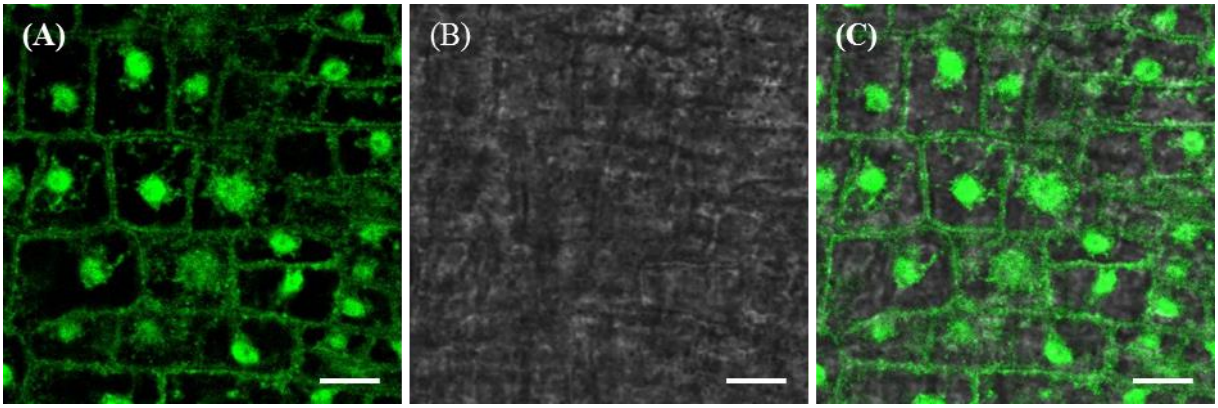

Figure 3.7. Sub-cellular localization of D14L protein

Cells in Expanding leaf blades of *p35S::D14L:GFP* (A) GFP fluorescence; (B) visible light; (C) merged images. bar = 100 μm

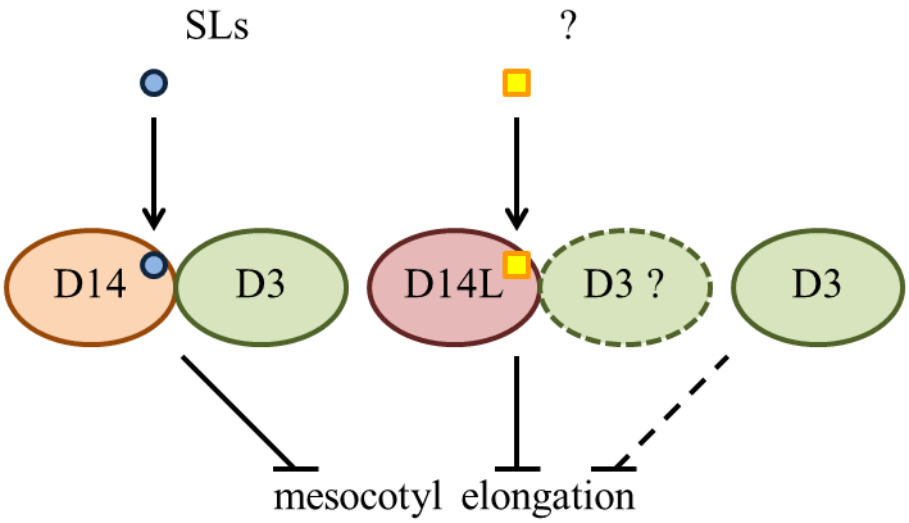

Figure 3.8. Model of *D14L* function in mesocotyl morphogenesis.

D14L functions additively with *D14* to suppress mesocotyl elongation under dark conditions. SL signaling is mediated by *D14* but not by *D14L*. *D3* functions with *D14* and probably with *D14L* to suppress mesocotyl elongation, and may also function in other pathways.

4. Expression of *DWARF14 LIKE2* is induced by arbuscular mycorrhizal fungi

4.1. Introduction

More than 80% of land plants have ability to form symbiotic association with arbuscular mycorrhizal (AM) fungi (Harrison, 2005). AM fungi help plants to uptake water and nutrients, such as phosphate and nitrate, while plants provide carbohydrate to AM fungi (Delaux et al., 2013).

During AM symbiosis, the fungal hyphae enter into the root and form highly specific structures called arbuscules. Therefore, for acceptance of AM fungi, plants have to suppress the defense response to hyphae and induce specific gene expression to form arbuscule (Delaux et al., 2013). The signaling molecules produced by AM fungi are called Myc factors, which trigger the AM symbiosis specific responses in plants (Fig. 4.1 A). The signal from the Myc factors is transduced by a series of genes called common symbiosis pathway (CSP) (Venkateshwaran et al., 2013) (Fig. 4.1 B).

Plants secrete SLs from roots. The secreted SLs enhance the symbiosis with AM fungi through induction of hyphal branching of AM fungi near the roots (Fig. 4.1 A) (Akiyama et al., 2005). Therefore, SL deficient mutants and a mutant of SL transporter show decreased colonization phenotypes (Gomez-Roldan et al., 2008; Koltai et al., 2010; Kretzschmar et al., 2012; Vogel et al., 2011). In contrast to the mutants of genes in CSP, no abnormal infection processes are observed in SL deficient mutants (Banba et al., 2008; Gutjahr et al., 2008; Yoshida et al., 2012). In addition, *d14* mutants showed an enhanced colonization phenotype probably due to an increased secretion of SLs by feedback regulation (Yoshida et al., 2012). These observations indicate that SL signaling

inside of plant root is not critical for the regulation of the AM fungi symbiosis.

Nonetheless, it was shown that the mutants in *D3*, another component of SL signaling pathway, exhibited a strongly reduced AM colonization and abnormal arbuscule formation phenotypes (Yoshida et al., 2012). Therefore, it is suggested that *D3* is required for AM fungus acceptance and that this function of *D3* is independent of SLs and *D14* (Fig. 4.1 A). However, how *D3* regulates AM fungus acceptance is largely unknown.

In this chapter, to examine how *D3* works for AM fungus acceptance, first, I examined if *D14L* is involved in this process, because it was implied that *D14L* and *D3* work together in a SL independent pathway as described in Chapter 3. It was shown that *D14L* is not involved in AM fungus acceptance. On the other hand, the expression of *D14L2a* and *D14L2b* is induced by the colonization of AM fungi (Hata unpublished results) (Fig. 4.2). Therefore, as a first step to elucidate the function of *D14L2a* and *D14L2b* in AM fungus acceptance, I analyzed the induction of *D14L2a* and *D14L2b* expression in AM symbiosis. I revealed that not CSP but *D3* is required for the induction of *D14L2a* and *D14L2b*.

4.2. Materials and methods

Plant and fungal materials

oscerk1, *ospollux*, and *d14-1*, *d3-2* were described previously (Arite et al., 2009; Banba et al., 2008; Miyata et al., 2014; Yoshida et al., 2012).

AM fungus *Rhizophagus irregularis* (previous name, *Glomus intraradices*) were

obtained from Premier Tech.

AM fungi infection

To observe *D14L* RNAi lines, rice seeds were sterilized in sodium hypochlorite and germinated in water for three days. These seedlings were transferred to autoclaved vermiculite containing about 1000 *Rhizophagus irregularis* spores. They were co-incubated for 35 days in an incubator (16h light, 8h dark at 25° C). Infected roots were stained with trypan blue as described by Banba et al., 2008, and were observed using a light microscope. Colonization percentages were evaluated using the magnified intersection method (Mcgonigle et al., 1990).

For other experiments, rice seeds were sterilized in sodium hypochlorite and germinated in water for three days. These seedlings were transferred to the soil (bottom layer, 20 g of Akadama soil (tuff loam) (Setogahara Kaen); upper layer; 45 g of Kanuma soil (weathered volcanic lapillus) / Ezo sand (small pumice) / Nippi soil (granular potting soil) (Nihon Hiryo) mixture (6:2:1, by weight)) containing about 1000 *Rhizophagus irregularis* spores. They were grown for 15 to 25 days in an incubator (15h light, 9h dark at 27° C). Water was supplied from the bottom by maintaining the water level at around 5mm.

Plasmid construction and transgenic rice production

To construct *pD14L2a::YFP*, ca. 3.4 kbp genome region including *D14L2a*

promoter and 5’ UTR was amplified using a primer set, D14L2a F and D14L2a R. Yellow fluorescence protein (YFP) sequence was amplified from the plasmid (Gene bank accession: gi:6009849) using a primer set, YFP F and YFP R. These fragments were sub-cloned into pBluescript SK vector. Subsequently, an NLS sequence (CCGGGCTGCAGCCTAAGAAGAAGAGAAAGGTTGGAGGATAGAGCT) was added to the C-terminal of YFP. *D14L2a* promoter and YFP-NLS fragment were cloned into pBI101.2 vector. Primer sets used for construction were described in Table 4.1.

Fluorescence microscopy

Roots co-incubated with AM fungi were fixed in 50% EtOH for 2 hour, and subsequently, in 20% KOH for 2 days at a room temperature. After washed with PBS buffer, fungal cell walls were stained with WGA-FITC (0.2 μM in PBS; Vector laboratories, Burlingame, CA, USA) for over-night. FITC and YFP florescence were observed under the microscope (Leica M165FC).

Quantitative reverse transcription-PCR

Total RNA was extracted from roots using Plant RNA Isolation kit (Agilent Technologies). After DNase I treatment, first-strand cDNA was synthesized using SuperScript III reverse transcriptase (Life Technologies). PCR was performed with SYBR green using Light Cycler 480 System II (Roche Applied Science, Penzberg, Germany). Primer sets used for qPCR were described in Table 4.1.

4.3. Results

4.3.1. *D14* and *D14L* are not required for AM symbiosis

In Chapter3, I showed that *D14L* functions in skotomorphogenesis in a SL independent manner. Based on the results that mesocotyl elongation in *d3* mutants was larger than that of *d14-1* and *D14L* RNAi lines, I proposed a working hypothesis that signaling pathways in which *D14* and *D14L* share *D3* as a common component in the two pathways. This idea promoted me to test a possibility that *D14L* works with *D3* to regulate AM symbiosis.

Plants of *D14L* RNAi lines in WT or *d14-1* background, described in Chapter 3, were co-incubated with AM fungi and the colonization rates were measured. As shown previously, the colonization of AM fungi was strongly suppressed in *d3* mutants (Fig. 4.3). On the other hand, the colonization rates of *D14L* RNAi lines in WT background were equivalent to WT plants (Fig. 4.3 A). *d14-1* mutant showed an enhanced colonization phenotype in consistent with the previous report (Fig. 4.3 B). It is likely that increased secretion of SL in *d14-1* by feedback regulation of SL biosynthesis led to the increase in AM fungi colonization. *D14L* RNAi line in *d14-1* background exhibited similar phenotype as *d14-1* mutants (Fig. 4.3 B). These results suggest that both *D14* and *D14L* are not required for AM symbiosis in contrary to my prediction.

4.3.2. Expression of *D14L2a* and *D14L2b* are induced by AM fungi colonization

The transcriptome analysis showed that the expression of two genes belonged to the

DLK2 subclade (*D14L2a* and *D14L2b*) were upregulated by AM colonization (Hata et al., unpublished results) (Fig. 4.2). To confirm this induction, I compared the expression levels of *D14* family genes in AM colonized and uncolonized roots. Induction of *AM1* and *AM3*, AM symbiosis marker genes, was observed in AM colonized roots (Gutjahr et al., 2008) (Fig. 4.4 A). Among four *D14* family genes, *D14L2a* and *D14L2b* were induced in AM colonized roots but no significant change were observed for *D14* and *D14L* (Fig. 4.4 B). Since the induction was stronger for *D14L2a*, spatial and temporal expression patterns of *D14L2a* at early stages of the AM colonization were examined by using *D14L2a* promoter::YFP-NLS lines. The YFP fluorescence was observed in five independent lines. In AM colonized roots, patchy induction of YFP fluorescence was observed in all lines (Fig. 4.4 C). This indicates that *D14L2a* expression is locally upregulated by AM fungi. The infection of hyphae was observed in some of the regions where YFP was induced, while the AM hyphae were not observed in the other region (Fig. 4.4 D). This result suggests that the expression of *D14L2a* is induced in early stages of AM colonization, prior to hyphal infection.

4.3.3. *D14L2a* and *D14L2b* are induced in a CSP independent but *D3* dependent pathway

To investigate the genetic pathways that control *D14L2a* and *D14L2b*, I first analyzed the relationship between the induction of these genes and CSP. *CERK1*, which is a candidate of the Myc-factor receptor, and *POLLUX*, which is a CSP component, work in AM symbiosis (Banba et al., 2008; Miyata et al., 2014, Zhang et al., 2015) (Fig.

4.1 B). The expression levels of AM symbiosis marker genes after the co-incubation with AM fungi were significantly lower in *cerk1* and *pollux* mutants compared to WT (Fig. 4.5 A). On the other hand, induction of *D14L2a* and *D14L2b* was still observed in these mutants (Fig. 4.5 B). This suggests that the induction of *D14L2a* and *D14L2b* by AM fungi depend on neither *CERK1* nor CSP. Next, I analyzed if *D3* is involved in the induction of *D14L2a* and *D14L2b*. WT plants and *d3-2* were co-incubated with AM fungi. In *d3-2* mutant, the expression of AM symbiosis marker genes was strictly suppressed as described previously (Yoshida et al., 2012) (Fig. 4.6 A). Likewise, the expression of *D14L2a* and *D14L2b* was inhibited in *d3-2* (Fig. 4.6 B). This result indicates that *D3* is required for the induction of *D14L2a* and *D14L2b* expression by AM fungi.

4.4. Discussion

The work performed by my collaborators and myself showed that *D3* is required for AM fungi acceptance whereas SLs and *D14* are not involved in that process (Yoshida et al., 2012). Since *D3* works in combination with *D14* family genes to regulate variable aspects of plant development, it is reasonable to presume that other *D14* family genes may function with *D3* in the process of AM fungi acceptance. In this study, it was suggested that *D14L* is also not involved in AM fungi acceptance. Currently, whether *D14L2a* and *D14L2b* are requires for AM fungi acceptance is still unclear. To clarify this point, it is crucial to determine AM fungi infection in *d14l2ad14l2b* double knock out mutants.

CSP was not required for the induction of *D14L2a* and *D14L2b* by AM fungi. On

the other hand, *D14L2a* and *D14L2b* were expressed under the control of *D3* function because induction of their expression by AM fungi was not observed in *d3* mutants. Considering that *D3* is required for AM fungi acceptance, these results imply that *D3* regulate AM fungi symbiosis in CSP independent manner. Moreover, since the signal from Myc-factors is thought to be transduced *via* CSP, results obtained in this study suggest that *DLK2* is induced by unknown signals derived from AM fungi (Fig. 4.7). Identification of components that work upstream and downstream of *D3* would lead to the discovery of a novel signaling pathway required for AM symbiosis.

Table 4.1. Primers used in Chapter 4

	name	sequence 5' → 3'
construction	D14L2a F	CCTAGGCTAGCTAGGACATATAAT
	D14L2a R	TCTAGAAGCTTCGATCAGCTATAG
	YFP F	TCTAGAATGGTGAGCAAGGGC
	YFP R	CCCGGGCTTGTACAGCTCGt
qPCR	D14 RT F9	CATCCGACGACCTGACCTC
	D14 RT R9	CGTGGTAGTCGCTGTCGTTC
	D14L RT F	TGGAGGATTTGAGCAGGAG
	D14L RT R	CACCAGGCCTTGTAGTTTGAC
	D14L2a RT F	CACCACAACCTCCTCCTCTT
	D14L2a RT R	GTCGCCGAGGAAGATCATCT
	D14L2b RT F	CTAGCCACTTGCCACTTCCA
	D14L2b RT R	ATGACGACCCAAACACGAAC
	AM1 RT F	ACCTCGCCAAAATATATGTATGCTATT
	AM1 RT R	TTTGCTTGCCACACGTTTTAA
	AM3 RT F	CTGTTGTTACATCTACGAATAAGGAGAAG
	AM3 RT R	CAACTCTGGCCGGCAAGT
	UBQ RT F	AGAAGGAGTCCACCCTCCACC
	UBQ RT R	GCATCCAGCACAGTAAAACACG

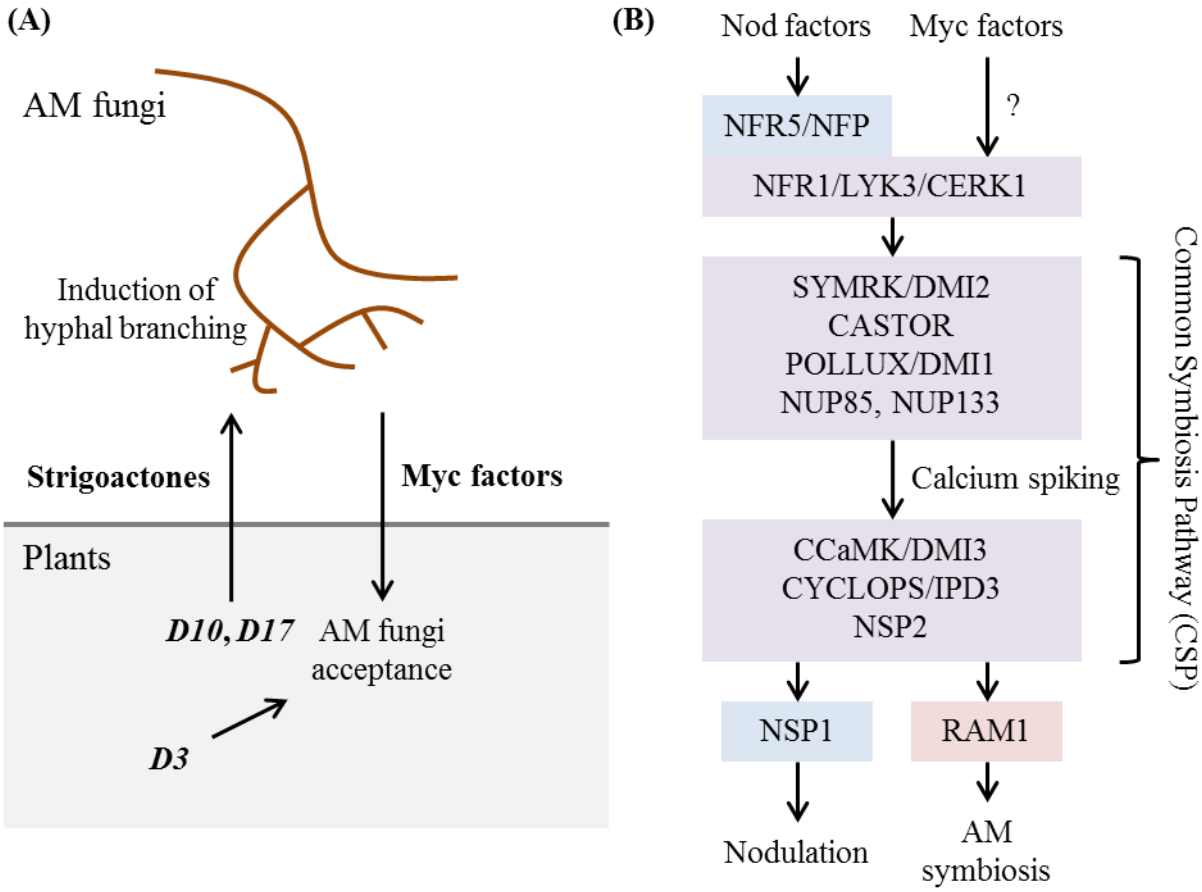

Figure 4.1. Interaction between plants and AM fungi

(A) Signaling molecules between plants and AM fungi. Plants secrete SLs to enhance hyphal branching in AM fungi, while AM fungi produce Myc factors to lead Plant responses for AM fungi acceptance. *D3* is required for AM fungi acceptance. (B) A schematic diagram of common symbiosis pathway (CSP). Genes in CSP function both in AM symbiosis and in nodulation. CERK1 is required for AM symbiosis and a candidate of Myc-factor receptor.

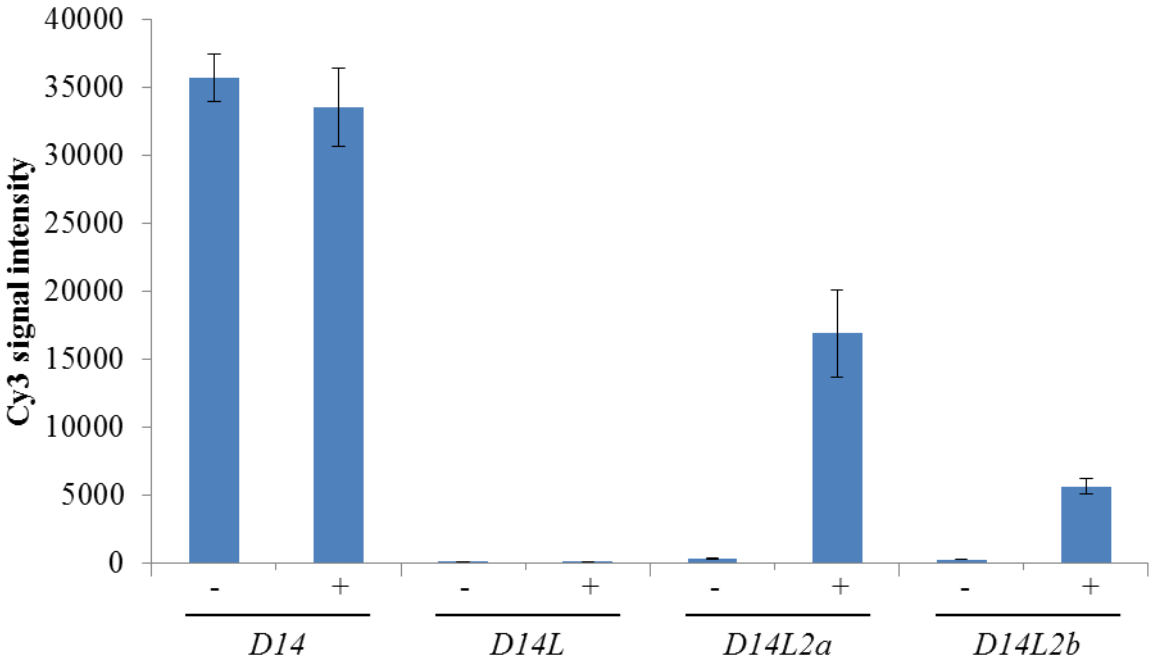

Figure 4.2. Expression of D14 family genes in AM symbiosis

Relative expression levels of *D14* family genes in AM colonized roots (+) and in uncolonized ones (-). This microarray analysis was done by Hata (unpublished). The expression of *D142a* and *D14L2b* was induced by AM fungi. Data are means ・ standard error. n = 3.

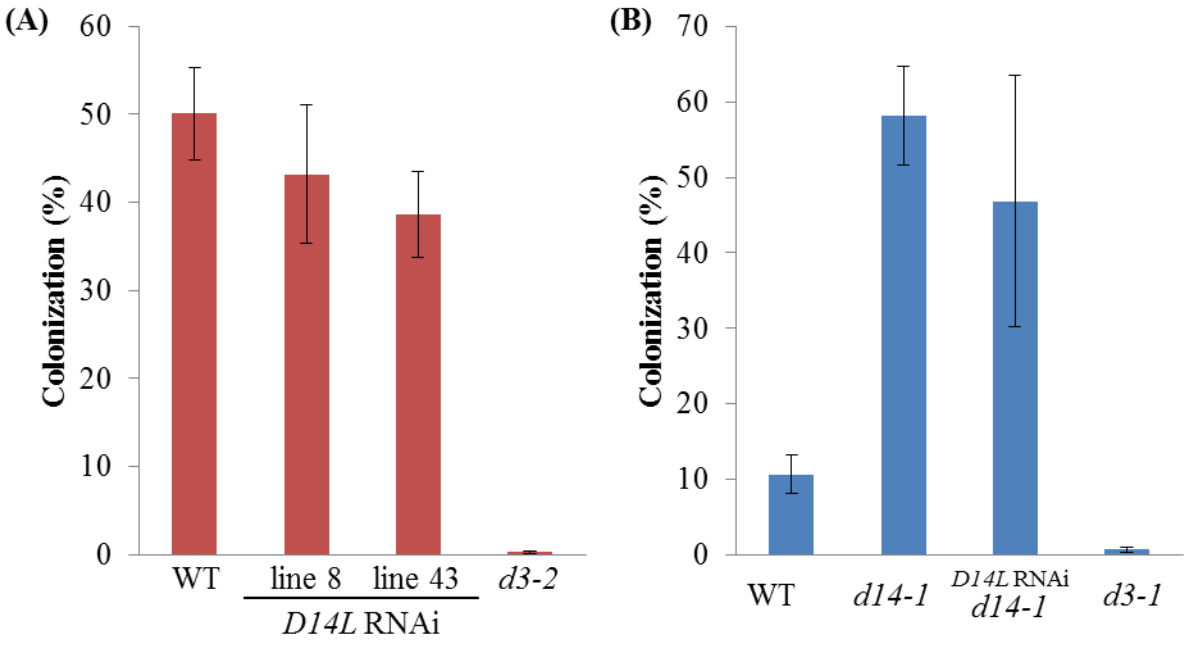

Figure 4.3. D14L is not required for AM fungi acceptance

The AM fungi colonization rates in Nipponbare background plants (A) and Shiokaribackground plants (B) at 5 wpi. The colonization rates of *D14L* RNAi lines in WT background and *d14-1* background are equivalent to WT and *d14-1*, respectively. Data are means ・ standard error. n = 2–11.

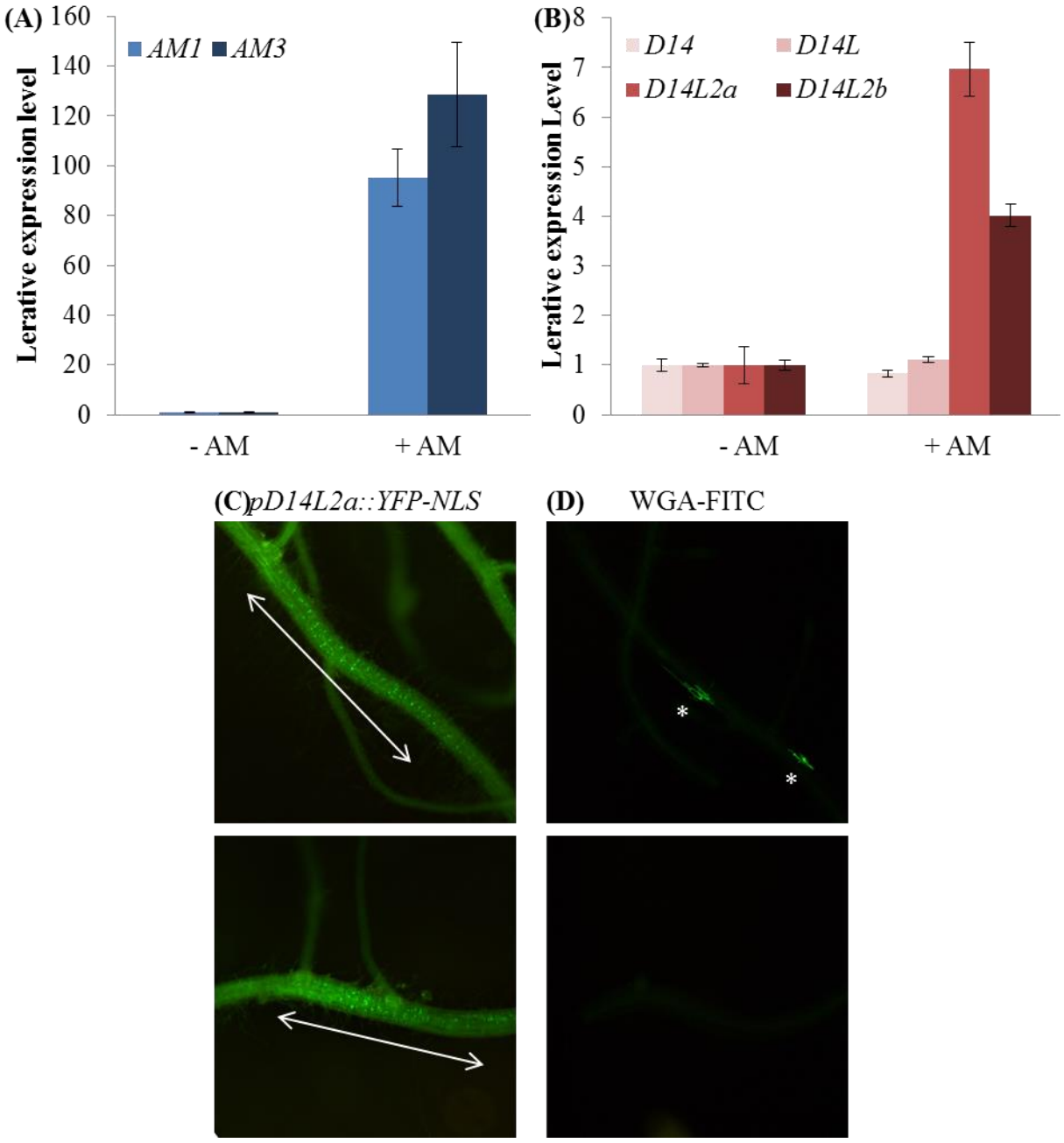

Figure 4.4. The expression of *D142a* and *D14L2b* is up-regulated by AM fungi

(A, B) The expression levels of AM symbiosis marker genes (A) and *D14* family genes (B) in colonized roots (15 dpi) compared with uncolonized ones. The expression of *D142a* and *D14L2b* were induced by AM fungi. Data are means ・ standard error. n = 3. (C) The expression of YFP in colonized roots of *pD14L2a::YFP-NLS* lines. (D) hyphae in YFP expressed region. Hyphae were stained with WGA-FITC. Hyphae were observed some of these regions but were not observed in the others.

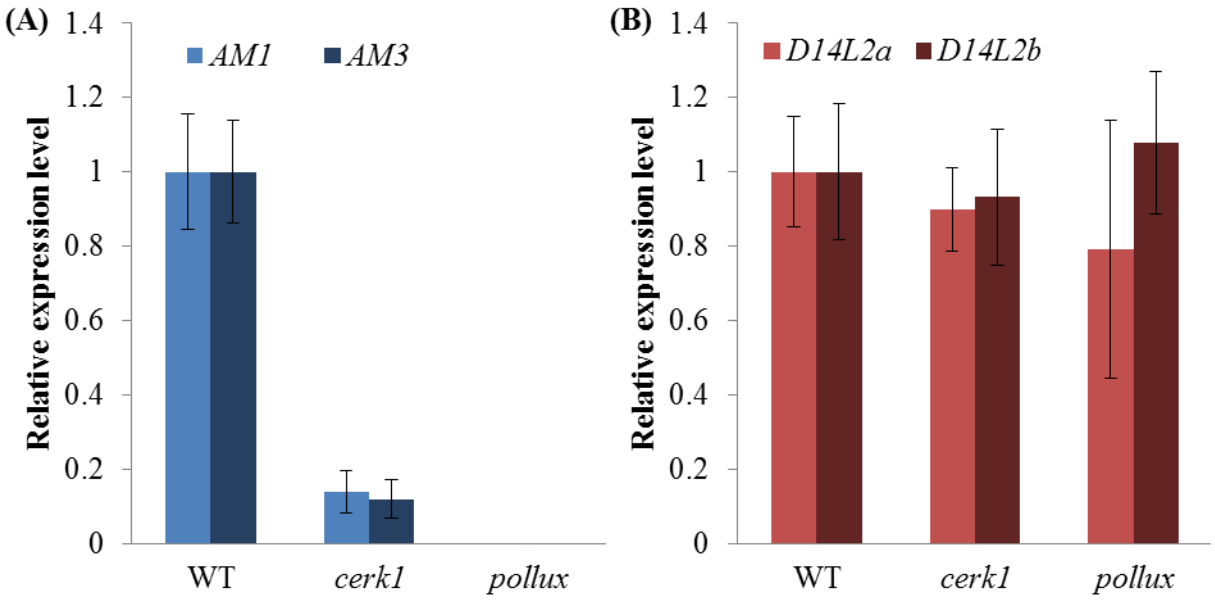

Figure 4.5. The expression of *D142a* and *D14L2b* were induced in CSP independent manner.

The expression levels of AM symbiosis marker genes (A) and *D142a* and *D14L2b* (B) in WT plants, *cerk1*, and *pollux* at 18 dpi. The expression levels of *D14L2a* and *D14L2b* in *cerk1* and *pollux* equivalent to those in WT plants. Data are means ・ standard error. n = 3.

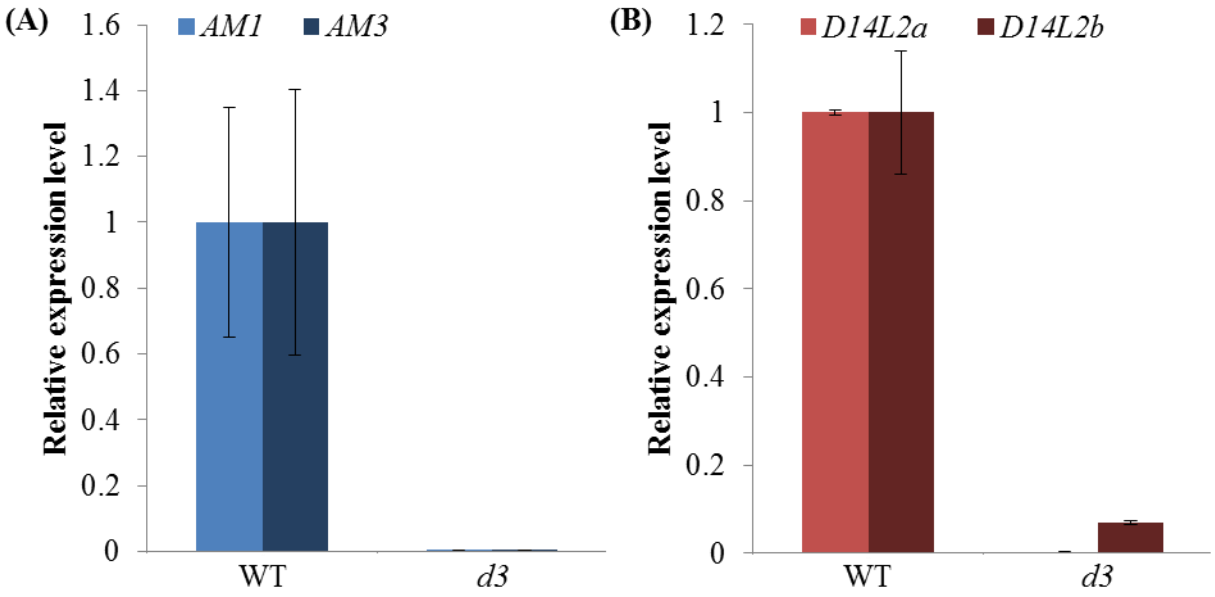

Figure 4.6. *D3* is required for the induction of *D142a* and *D14L2b* by AM fungi.
The expression levels of AM symbiosis marker genes (A) and *D142a* and *D14L2b* genes (B) in WT plants and *d3* at 25 dpi. The expression *D142a* and *D14L2b* were inhibited in *d3*. Data are means ・ standard error. n = 3.

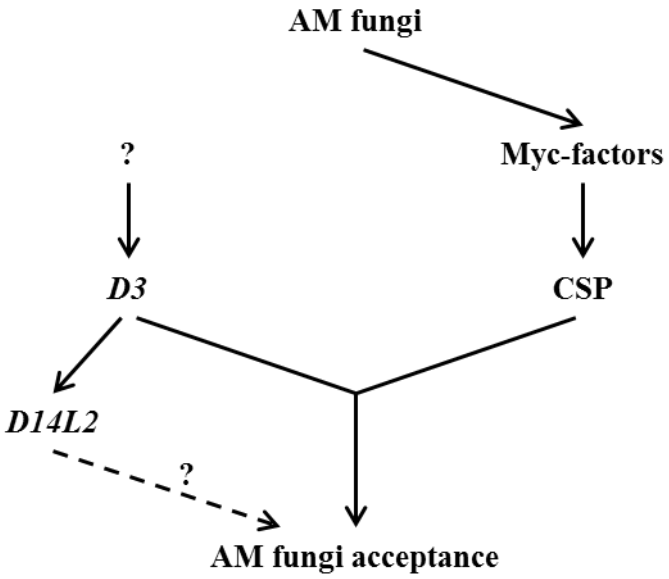

Figure 4.7. Model of *D3* and *D14L2* functions in AM fungi acceptance.
Both *D3* and CSP are required for AM fungi acceptance. CSP is involved in Myc-facter signaling, while *D3* may transduce unknown signaling. *D14L2a* and *D14L2b* are in the downstream of *D3* but not of CSP. It is unclear whether *D14L2a* and *D14L2b* are required for AM fungi acceptance.

5. General discussion

I clarified the intercellular transport of D14 protein through phloem. The proteome analysis performed by Aki et al. (2008) and Batailler et al. (2012) suggested that D14 family proteins are contained in phloem sap in rice and Arabidopsis. Considering these results together, it is implied that the ability to move between cells is conserved among D14 family proteins. In order to control plant hormone signaling, components in the signaling pathways are regulated at various levels, such as transcription, translation, subcellular localization and protein degradation (Chevalier et al., 2014; Marin et al., 2010; Pérez-Torres et al., 2008; Russinova et al., 2004). In addition to these known types of regulation, my study showed a possibility that the intercellular transport of hormone signaling components works as a novel way to modulate plant hormone signaling and the action of hormones.

My work indicated that *D14* family genes play different roles in the control of rice growth and development. In addition, not all phenotypes of *d3* mutants are observed in SL deficient mutants. This suggests that *D3* mediates not only the SL signal but also other unknown signals. A possible explanation for these observations is that each of the *D14* family genes contributes to the *D3* function in a distinctive way rather than redundantly. The fact that genes in all of *D14*, *D14L*, and *DLK2* clades are conserved in seed plants supports a hypothesis that the individual clade plays specific roles (Delaux et al. 2012; Waters et al., 2012). Considering that D14 is the putative SL receptor, it is possible that the other D14 family proteins bind to ligands and work as receptors. So far, the plant hormone receptor family whose paralogous genes perceive different hormones has not been discovered.

In this thesis, I characterized the novel features and functions of *D14* family genes. These findings will be valuable basis to further elucidate the ability of plants to adapt to changeable environments.

Acknowledgements

Foremost, I would like to express my sincere gratitude to Dr. Junko Kyozuka for her guidance, support, and suggestion throughout this study. I also express my gratitude to Professor Nobuhiro Tsutsumi, Drs. Junichi Ito, Shinichi Arimura, and Koji Yamaji for their critical comments to complete this thesis. I am grateful to Professors Christine Beveridge, Catherine Rameau, Drs. Elizabeth Dun, Philip Brewer, Alexandre de Saint Germain, and Mauricio Lopez-Obando for the collaboration corresponding to Chapter 2. I am also grateful to Professors Shingo Hata, Toru Fujiwara, and Dr. Yoshihiro Kobae for the collaboration corresponding to Chapter 4. I acknowledge Professor Jianfeng Ma and Dr. Naoki Yamaji for their support of immune staining experiments. I express my gratitude to Professor Koki Akiyama, Ms. Misaki Tenpo, and their laboratory members for their support of the experiments about arbuscular mycorrhizal fungi. I thank Professor Mikio Nakazono and Dr. Zhongyuan Hu for their advice on the experiments about mesocotyl. I would like to thank all the members of my laboratory, the Laboratory of Crop Ecology and Morphology, for their kind support. Finally, I would like to express my sincere gratitude to my families, grandparents, and all friends for their continuous supports and encouragements throughout my study.

References

Abe,S., Sado, A., Tanaka, K., Kisugi, T., Asami, K., Ota, S., Kim, H.I., Yoneyama, K., Xie, X., Ohnishi, T., Seto,Y., Yamaguchi, S., Akiyama, K., Yoneyama, K., Nomura, T., 2014. Carlactone is converted to carlactonoic acid by MAX1 in *Arabidopsis* and its methyl ester can directly interact with AtD14 in vitro. Proc. Natl. Acad. Sci. USA. 111, 18084-18089.

Aki, T., Shigyo, M., Nakano, R., Yoneyama, T., Yanagisawa, S., 2008. Nano scale proteomics revealed the presence of regulatory proteins including three FT-Like proteins in phloem and xylem saps from rice. Plant Cell Physiol. 49, 769-790.

Alder, A., Jamil, M., Marzorati, M., Bruno, M., Vermathen, M., Bigler, P., Ghisla, S., Bouwmeester, H., Beyer, P., Al-Babili, S., 2012. The path from β-carotene to carlactone, a strigolactone-like plant hormone. Science. 335, 1348-1351.

Arite, T., Kameoka, H., Kyozuka, J., 2012. Strigolactone positively controls crown root elongation in rice. J. Plant Growth Regul. 31, 165-172.

Arite, T., Umehara, M., Ishikawa, S., Hanada, A., Maekawa, M., Yamaguchi, S., Kyozuka, J., 2009. *d14*, a strigolactone-insensitive mutant of rice, shows an accelerated outgrowth of tillers. Plant Cell. Physiol. 50, 1416-1424.

Bainbridge, K., Sorefan, K., Ward, S., Leyser, O., 2005. Hormonally controlled expression of the Arabidopsis *MAX4* shoot branching regulatory gene. Plant J. 44, 569-580.

Banba, M., Gutjahr, C., Miyao, A., Hirochika, H., Paszkowski, U., Kouchi, H., Imaizumi-Anraku, H., 2008. Divergence of evolutionary ways among common *sym* genes: CASTOR and CCaMK show functional conservation between two symbiosis systems and constitute the root of a common signaling pathway. Plnat Cell Physiol.

49, 1659-1671.

Batailler, B., Lemaître, T., Vilaine, F., Sanchez, C., Renard, D., Cayla, T., Beneteau, J., Dinant, S., 2012. Soluble and filamentous proteins in *Arabidopsis* sieve elements. Plant Cell Environ. 35, 1258-1273.

Beveridge, C.A., Ross, J.J., Murfet, I.C., 1996. Branching in Pea (Action of Genes *Rms3* and *Rms4*). Plant Physiol. 110, 859-865.

Bloemendal, S., Kück, U., 2013. Cell-to-cell communication in plants, animals, and fungi: a comparative review. Naturwissenschaften. 100, 3-19.

Booker, J., Auldridge, M., Wills, S., McCarty, D., Klee, H. and Leyser, O., 2004. MAX3/CCD7 is a carotenoid cleavage dioxygenase required for the synthesis of a novel plant signaling molecule. Curr. Biol. 14, 1232-1238.

Booker, J., Sieberer, T., Wright, W., Williamson, L., Willett, B., Stirnberg, P., Turnbull, C., Srinivasan, M., Goddard, P., Leyser, O., 2005. *MAX1* encodes a cytochrome P450 family member that acts downstream of *MAX3/4* to produce a carotenoid-derived branch-inhibiting hormone. Dev. Cell. 8, 443-449.

Chang, C.C., Huang, P.S., Lin, H.R., Lu, C.H., 2007. Transactivation of protein expression by rice HSP101 in planta and using *Hsp101* as a selection marker for transformation. Plnat Cell Physiol. 48, 1098-1107.

Chevalier, F., Nieminen, K., Sánchez-Ferrero, J.C., Rodríguez, M.L., Chagoyen, M., Hardtke, C.S., Cubas, P., 2014. Strigolactone promotes degradation of DWARF14, an α/β hydrolase essential for strigolactone signaling in Arabidopsis. Plant Cell. 26, 1134-1150.

de Jong, M., George, G., Ongaro, V., Williamson, L., Willetts, B., Ljung, K., McCulloch, H., Leyser, O., 2014. Auxin and strigolactone signaling are required for modulation

of Arabidopsis shoot branching by nitrogen supply. Plant Physiol. 166, 384-395.

De Storme, N., Geelen, D., 2014. Callose homeostasis at plasmodesmata: molecular regulators and developmental relevance. Front. Plant Sci. 5, 138.

Delaux ,P.M., Séjalon-Delmas, N., Bécard, G., Ané, J.M., 2013. Evolution of the plant-microbe symbiotic 'toolkit'. Trends. Plant. Sci. 18, 298-304.

Delaux, P.M., Xie, X., Timme, R.E., Puech-Pages, V., Dunand, C., Lecompte, E., Delwiche, C.F., Yoneyama, K., Bécard, G., Séjalon-Delmas, N., 2012. Origin of strigolactones in the green lineage. New Phytol. 195, 857-871.

Endo, S., Betsuyaku, S., Fukuda, H., 2014. Endogenous peptide ligand-receptor systems for diverse signaling networks in plants. Curr. Opin. Plant Biol. 21, 140-146.

Fisher, D.B., Cash-Clark, C.E., 2000. Sieve tube unloading and post-phloem transport of fluorescent tracers and proteins injected into sieve tubes via severed aphid stylets. Plant Physiol. 123, 125-128.

Flematti, G.R., Ghisalberti, E.L., Dixon, K.W., Trengove, R.D., 2004. A compound from smoke that promotes seed germination. Science. 305, 977.

Foo, E., Turnbull, C.G., Beveridge, C.A., 2001. Long-distance signaling and the control of branching in the *rms1* mutant of pea. Plant Physiol. 126, 203-209.

Furuta, K.M., Yadav, S.R., Lehesranta, S., Belevich, I., Miyashima, S., Heo, J.O., Vatén, A., Lindgren, O., De Rybel, B., Van Isterdael, G., Somervuo, P., Lichtenberger, R., Rocha, R., Thitamadee, S., Tähtiharju, S., Auvinen, P., Beeckman, T., Jokitalo, E., Helariutta, Y., 2014. Plant development. Arabidopsis NAC45/86 direct sieve element morphogenesis culminating in enucleation. Science. 345, 933-937.

González-Grandío, E., Poza-Carrión, C., Sorzano, C.O., Cubas, P., 2013. *BRANCHED1* promotes axillary bud dormancy in response to shade in *Arabidopsis*. Plant Cell. 25,

834-850.

Gomez-Roldan, V., Fermas, S., Brewer, P.B., Puech-Pagès, V., Dun, E.A., Pillot, J.P., Letisse, F., Matusova, R., Danoun, S., Portais, J.C., Bouwmeester, H., Bécard, G., Beveridge, C.A., Rameau, C., Rochange, S.F., 2008. Strigolactone inhibition of shoot branching. Nature. 455, 189-194.

Guo, Y., Zheng, Z., La Clair, J.J., Chory, J., Noel, J.P., 2013. Smoke-derived karrikin perception by the α/β-hydrolase KAI2 from Arabidopsis. Proc. Natl. Acad. Sci. USA. 110, 8284-8289.

Gutjahr, C., Banba, M., Croset, V., An, K., Miyao, A., An, G., Hirochika, H., Imaizumi-Anraku, H., Paszkowski, U., 2008. Arbuscular mycorrhiza-specific signaling in rice transcends the common symbiosis signaling pathway. Plant Cell 20, 2989-3005.

Hamiaux, C., Drummond, R.S., Janssen, B.J., Ledger, S.E., Cooney, J.M., Newcomb, R.D., Snowden, K.C., 2012. DAD2 is an α/β hydrolase likely to be involved in the perception of the plant branching hormone, strigolactone. Curr. Biol. 22, 2032-2036.

Han, X., Kumar, D., Chen, H., Wu, S., Kim, J.Y., 2014. Transcription factor-mediated cell-to-cell signalling in plants. J. Exp. Bot. 65, 1737-1749.

Harrison, M.J., 2005. Signaling in the arbuscular mycorrhizal symbiosis. Annu. Rev. Microbiol. 59, 19-42.

Hisanaga, T., Miyashima, S., Nakajima, K., 2014. Small RNAs as positional signal for pattern formation. Curr. Opin. Plant. Biol. 21, 37-42.

Hu, Z., Yamauchi, T., Yang, J., Jikumaru, Y., Tsuchida-Mayama, T., Ichikawa, H., Takamure, I., Nagamura, Y., Tsutsumi, N., Yamaguchi, S., Kyozuka, J., Nakazono, M., 2014. Strigolactone and cytokinin act antagonistically in regulating rice

mesocotyl elongation in darkness. Plant Cell Physiol. 55, 30-41

Hu, Z., Yan, H., Yang, J., Yamaguchi, S., Maekawa, M., Takamure, I., Tsutsumi, N., Kyozuka, J., Nakazono, M., 2010. Strigolactones negatively regulate mesocotyl elongation in rice during germination and growth in darkness. Plant Cell Physiol. 51, 1136-1142.

Ishikawa, S., Maekawa, M., Arite, T., Onishi, K., Takamure, I., Kyozuka, J., 2005. Suppression of tiller bud activity in tillering dwarf mutants of rice. Plant Cell Physiol. 46, 79-86.

Jiang, L., Liu, X., Xiong, G., Liu, H., Chen, F., Wang, L., Meng, X., Liu, G., Yu, H., Yuan, Y., Yi, W., Zhao, L., Ma, H., He, Y., Wu, Z., Melcher, K., Qian, Q., Xu, HE., Wang, Y., Li, J., 2013. DWARF 53 acts as a repressor of strigolactone signalling in rice. Nature. 504, 401-405.

Johnson, X., Brcich, T., Dun, E.A., Goussot, M., Haurogné, K., Beveridge, C.A., Rameau, C., 2006. Branching genes are conserved across species. Genes controlling a novel signal in pea are coregulated by other long-distance signals. Plant Physiol. 142, 1014-1026.

Kapulnik, Y., Delaux, P.M., Resnick, N., Mayzlish-Gati, E., Wininger, S., Bhattacharya, C., Séjalon-Delmas, N., Combier, J.P., Bécard, G., Belausov, E., Beeckman, T., Dor, E., Hershenhorn, J., Koltai, H., 2011. Strigolactones affect lateral root formation and root-hair elongation in *Arabidopsis*. Planta. 233, 209-216.

Kebrom, T.H., Brutnell, T.P., Finlayson, S.A., 2010. Suppression of sorghum axillary bud outgrowth by shade, phyB and defoliation signalling pathways.

Koltai, H., LekKala, S.P., Bhattacharya, C., Mayzlish-Gati, E., Resnick, N., Wininger, S., Dor, E., Yoneyama, K., Yoneyama, K., Hershenhorn, J., Joel, D.M., Kapulnik, Y.,

2010. A tomato strigolactone-impaired mutant displays aberrant shoot morphology and plant interactions. J. Exp. Bot. 61, 1739-1749.

Kouchi, H., Sekine, M., Hata, S., 1995. Distinct classes of mitotic cyclins are differentially expressed in the soybean shoot apex during the cell cycle. Plant Cell. 7, 1143-1155.

Kretzschmar, T., Kohlen, W., Sasse, J., Borghi, L., Schlegel, M., Bachelier, J.B., Reinhardt, D., Bours, R., Bouwmeester, H.J., Martinoia, E., 2012. A petunia ABC protein controls strigolactone-dependent symbiotic signalling and branching. Nature. 483, 341-344.

Lin, H., Wang, R., Qian, Q., Yan, M., Meng, X., Fu, Z., Yan, C., Jiang, B., Su, Z., Li, J., Wang, Y., 2009. DWARF27, an iron-containing protein required for the biosynthesis of strigolactones, regulates rice tiller bud outgrowth. Plant Cell. 21, 1512-1525

Liu, L., Zhu, Y., Shen, L., Yu, H., 2013. Emerging insights into florigen transport. Curr. Opin. Plant Biol. 16, 607-613.

Marin, E., Jouannet, V., Herz, A., Lokerse, A.S., Weijers, D., Vaucheret, H., Nussaume, L., Crespi, M.D., Maizel, A., 2010. miR390, *Arabidopsis TAS3* tasiRNAs, and their *AUXIN RESPONSE FACTOR* targets define an autoregulatory network quantitatively regulating lateral root growth.

Mayzlish-Gati, E., De-Cuyper, C., Goormachtig, S., Beeckman, T., Vuylsteke, M., Brewer, P.B., Beveridge, C.A., Yermiyahu, U., Kaplan, Y., Enzer, Y., Wininger, S., Resnick, N., Cohen, M., Kapulnik, Y., Koltai, H., 2012. Strigolactones are involved in root response to low phosphate conditions in Arabidopsis. Plant Physiol. 160, 1329-1341.

McGonigle, T.P., Miller, M.H., Evans, D.G., Fairchild, G. L., Swan, J. A., 1990. A new

method which gives an objective measure of colonization of roots by vesicular-arbuscular mycorrhizal fungi. New Phytol. 115, 495-501.

Miyata, K., Kozaki, T., Kouzai, Y., Ozawa, K., Ishii, K., Asamizu, E., Okabe, Y., Umehara, Y., Miyamoto, A., Kobae, Y., Akiyama, K., Kaku, H., Nishizawa, Y., Shibuya, N., Nakagawa, T., 2014. The Bifunctional Plant Receptor, OsCERK1, Regulates Both Chitin-Triggered Immunity and Arbuscular Mycorrhizal Symbiosis in Rice. Plant Cell Physiol. 55, 1864-1872.

Morris, S.E., Turnbull, C.G., Murfet, I.C., Beveridge, C.A., 2001. Mutational analysis of branching in pea. Evidence that *Rms1* and *Rms5* regulate the same novel signal. Plant Physiol. 126, 1205-1213.

Nakagawa, M., Shimamoto, K., Kyozuka, J., 2002. Overexpression of *RCN1* and *RCN2*, rice *TERMINAL FLOWER 1/CENTRORADIALIS* homologs, confers delay of phase transition and altered panicle morphology in rice. Plant J. 29, 743-50.

Nakagawa, T., Kurose, T., Hino, T., Tanaka, K., Kawamukai, M., Niwa, Y., Toyooka, K., 2007. Development of series of gateway binary vectors, pGWBs, for realizing efficient construction of fusion genes for plant transformation. J. Biosci. Bioeng. 104, 34-41.

Nelson, D.C., Flematti, G.R., Riseborough, J.A., Ghisalberti, E.L., Dixon, K.W., Smith, S.M., 2010. Karrikins enhance light responses during germination and seedling development in *Arabidopsis thaliana*. Proc. Natl. Acad. Sci. USA. 107, 7095-7100.

Nelson, D.C., Scaffidi, A., Dun, E.A., Waters, M.T., Flematti, G.R., Dixon, K.W., Beveridge, C.A., Ghisalberti, E.L., Smith, S.M., 2011. F-box protein MAX2 has dual roles in karrikin and strigolactone signaling in Arabidopsis thaliana. Proc. Natl. Acad. Sci. USA. 108, 8897-8902.

Osuna, D., Usadel, B., Morcuende, R., Gibon, Y., Bläsing, O.E., Höhne, M., Günter, M., Kamlage, B., Trethewey, R., Scheible, W.R., Stitt, M., 2007. Temporal responses of transcripts, enzyme activities and metabolites after adding sucrose to carbon-deprived Arabidopsis seedlings. Plant J. 49, 463-91.

Pérez-Torres, C.A., López-Bucio, J., Cruz-Ramírez, A., Ibarra-Laclette, E., Dharmasiri, S., Estelle, M., Herrera-Estrella, L., 2008. Phosphate availability alters lateral root development in Arabidopsis by modulating auxin sensitivity via a mechanism involving the TIR1 auxin receptor. Plant Cell. 20, 3258-3272.

Rasmussen, A., Mason, M.G., De Cuyper, C., Brewer, P.B., Herold, S., Agusti, J., Geelen, D., Greb, T., Goormachtig, S., Beeckman, T., Beveridge, C.A., 2012. Strigolactones suppress adventitious rooting in Arabidopsis and pea. Plant Physiol. 158, 1976-87.

Russinova, E., Borst, J.W., Kwaaitaal, M., Caño-Delgado, A., Yin, Y., Chory, J., de Vries, S.C., 2004. Heterodimerization and endocytosis of Arabidopsis brassinosteroid receptors BRI1 and AtSERK3 (BAK1). Plant Cell. 16, 3216-3229.

Ruyter-Spira, C., Kohlen, W., Charnikhova, T., van Zeijl, A., van Bezouwen, L., de Ruijter, N., Cardoso, C., Lopez-Raez, J.A., Matusova, R., Bours, R., Verstappen, F., Bouwmeester, H., 2011. Physiological effects of the synthetic strigolactone analog GR24 on root system architecture in Arabidopsis: another belowground role for strigolactones? Plant Physiol. 155, 721-734.

Santner, A., Calderon-Villalobos, L., Estelle, M., 2009. Plant hormones are versatile chemical regulators of plant growth. Nat. Chem. Biol. 5, 301-307.

Scaffidi, A., Waters, M.T., Ghisalberti, E.L., Dixon, K.W., Flematti, G.R., Smith, S.M., 2013. Carlactone-independent seedling morphogenesis in Arabidopsis. Plant J. 76,

1-9.

Scaffidi, A., Waters, M.T., Sun, Y.K., Skelton, B.W., Dixon, K.W., Ghisalberti, E.L., Flematti, G.R., Smith, S.M., 2014. Strigolactone Hormones and Their Stereoisomers Signal through Two Related Receptor Proteins to Induce Different Physiological Responses in Arabidopsis. Plant Physiol. 165, 1221-1232.

Seto Y, Kameoka H, Yamaguchi S, Kyozuka J. 2012. Recent advances in strigolactone research: chemical and biological aspects. Plant Cell Phisiol. 53, 1843-1853.

Seto, Y., Sado, A., Asami, K., Hanada, A., Umehara, M., Akiyama, K., Yamaguchi, S., 2014. Carlactone is an endogenous biosynthetic precursor for strigolactones. Proc. Natl. Acad. Sci. USA. 111, 1640-1645.

Shen, H., Luong, P., Huq, E., 2007. The F-box protein MAX2 functions as a positive regulator of photomorphogenesis in Arabidopsis. Plant Physiol. 145, 1471-1483.

Shen, H., Zhu, L., Bu, Q.Y., Huq, E., 2012. MAX2 Affects Multiple Hormones to Promote Photomorphogenesis. Mol. Plant. 5, 750-762.

Simons, J.L., Napoli, C.A., Janssen, B.J., Plummer, K.M., Snowden, K.C., 2007. Analysis of the *DECREASED APICAL DOMINANCE* genes of petunia in the control of axillary branching. Plant physiol. 143, 697-706

Stanga, J.P., Smith, S.M., Briggs, W.R., Nelson, D.C., 2013. *SUPPRESSOR OF MORE AXILLARY GROWTH2 1* controls seed germination and seedling development in Arabidopsis. Plant Physiol. 163, 318-330.

Stirnberg, P., van De Sande, K. and Leyser, H.M.O., 2002. *MAX1* and *MAX2* control shoot lateral branching in *Arabidopsis*. Development. 129, 1131-1141.

Su, H., Abernathy, S.D., White, R.H., Finlayson, S.A., 2011. Photosynthetic photon flux density and phytochrome B interact to regulate branching in Arabidopsis. Plant Cell

Environ. 34, 1986-1998.

Sun, X.D., Ni, M., 2010. HYPOSENSITIVE TO LIGHT, an alpha/beta fold protein, acts downstream of ELONGATED HYPOCOTYL 5 to regulate seedling de-etiolation. Mol. Plant. 4, 116-126.

Turgeon, R., Wolf, S., 2009. Phloem transport: cellular pathways and molecular trafficking. Annu. Rev. Plant Biol. 60, 207-221. A small-molecule screen identifies new functions for the plant hormone strigolactone. Nat. Chem. Biol. 6, 741-749.

Umehara, M., Hanada, A., Magome, H., Takeda-Kamiya, N., Yamaguchi, S., 2010. Contribution of strigolactones to the inhibition of tiller bud outgrowth under phosphate deficiency in rice. Plant Cell Physiol. 51, 1118-1126.

Umehara, M., Hanada, A., Yoshida, S., Akiyama, K., Arite, T., Takeda-Kamiya, N., Magome, H., Kamiya, Y., Shirasu, K., Yoneyama, K., Kyozuka, J., Yamaguchi, S., 2008. Inhibition of shoot branching by new terpenoid plant hormones. Nature. 455, 195-200.

Venkateshwaran, M., Volkening, J.D., Sussman, M.R., Ané, J.M., 2013. Symbiosis and the social network of higher plants. Curr. Opin. Plant Biol. 16, 118-127.

Vogel, J.T., Walter, M.H., Giavalisco, P., Lytovchenko, A., Kohlen, W., Charnikhova, T., Simkin, A.J., Goulet, C., Strack, D., Bouwmeester, H.J., Fernie, A.R., Klee, H.J., 2010. SlCCD7 controls strigolactone biosynthesis, shoot branching and mycorrhiza-induced apocarotenoid formation in tomato. Plant J. 61, 300-311.

Waters, M.T., Nelson, D.C., Scaffidi, A., Flematti, G.R., Sun, Y.K., Dixon, K.W. and Smith, S.M., 2012. Specialisation within the DWARF14 protein family confers distinct responses to karrikins and strigolactones in *Arabidopsis*. Development.139, 1285-1295.

Whipple, C.J., Kebrom, T.H., Weber, A.L., Yang, F., Hall, D., Meeley, R., Schmidt, R., Doebley, J., Brutnell, T.P., Jackson, D.P., 2011. *grassy tillers1* promotes apical dominance in maize and responds to shade signals in the grasses. Proc. Natl. Acad. Sci. USA. 16, 108, E506-E512.

Xie, X., Wang, G., Yang, L., Cheng, T., Gao, J., Wu, Y., Xia, Q., 2014. Cloning and characterization of a novel Nicotiana tabacum ABC transporter involved in shoot branching. Physiol. Plant. 2015. In press

Yamada, Y., Furusawa, S., Nagasaka, S., Shimomura, K., Yamaguchi, S., Umehara, M., 2014. Strigolactone signaling regulates rice leaf senescence in response to a phosphate deficiency. Planta. 240, 399-408.

Yamaji, N., Ma, J. F., 2007. Spatial Distribution and Temporal Variation of the Rice Silicon Transporter Lsi1. Plant Physiol. 143, 1306-1313.

Yoshida, S., Kameoka, H., Tempo, M., Akiyama, K., Umehara, M., Yamaguchi, S., Hayashi, H., Kyozuka, J., Shirasu, K., 2012. The D3 F-box protein is a key component in host strigolactone responses essential for arbuscular mycorrhizal symbiosis. New Phytol. 196, 1208-1216.

Zhang, X., Dong, W., Sun, J., Feng, F., Deng, Y., He, Z., Oldroyd, G.E., Wang, E., 2015. The receptor kinase CERK1 has dual functions in symbiosis and immunity signalling. Plant J. 81, 258-267.

Zhang, Y., van Dijk, A.D., Scaffidi, A., Flematti, G.R., Hofmann, M., Charnikhova, T., Verstappen, F., Hepworth, J., van der Krol, S., Leyser, O., Smith, S.M., Zwanenburg, B., Al-Babili, S., Ruyter-Spira, C., Bouwmeester, H.J., 2014b. Rice cytochrome P450 MAX1 homologs catalyze distinct steps in strigolactone biosynthesis. Nat. Chem. Biol. 10, 1028-1033.

Zhou, F., Lin, Q., Zhu, L., Ren, Y., Zhou, K., Shabek, N., Wu, F., Mao, H., Dong, W., Gan, L., Ma, W., Gao, H., Chen, J., Yang, C., Wang, D., Tan, J., Zhang, X., Guo, X., Wang, J., Jiang, L., Liu, X., Chen, W., Chu, J., Yan, C., Ueno, K., Ito, S., Asami, T., Cheng, Z., Wang, J., Lei, C., Zhai, H., Wu, C., Wang, H., Zheng, N., Wan, J., 2013. D14-SCF(D3)-dependent degradation of D53 regulates strigolactone signalling. Nature. 504, 406-410.